

Effects of the Pion Detector Shielding for the Moller Experiment (II)

Neven Simicevic*
Center for Applied Physics Studies
Louisiana Tech University, PO Box 10348, Ruston, LA 71272

Abstract

In this report detailed studies of the shielding properties and the physical consequences of the shielding of the pion detector are performed for the 1.8 GeV electrons and pions energies in the Moller experiment. Effects of the shielding on both, pion detector and the main detector system, are calculated for the lead shielding thicknesses of 20 and 50 cm. The type, the energy distributions and the rates of the secondary particles are computed. In addition to help optimize the thickness of the shielding, the results will help to understand the consequences of the background produced by the shielding on both, pion detector and the main detector system, and, therefore, help in the design of the detectors. The result can be also used to estimate the secondary particles effects on the main detector system if one decides to put the shielding in front of main detectors.

* Address correspondence at Louisiana Tech University, PO Box 10348, Ruston, LA 71272

Tel: 1.318.257.3591
Fax: 1.318.257.4228
E-mail: neven@phys.latech.edu

I. Introduction

Moller experiment proposes to measure the parity-violating asymmetry in the scattering of longitudinally polarized 11 GeV electrons from the atomic electrons in a liquid hydrogen target [MOLLER 2012].

Nominal design parameters for the proposed measurement are shown in Table 1. While some of the design parameters could change in the future at the few percentage level as the design is further optimized, possible changes are not important for the scope of this report.

Parameter	Value
E [GeV]	≈ 11.0
E' [GeV]	1.8 - 8.8
θ_{cm}	46° - 127°
θ_{lab}	0.23° - 1.1°
$\langle Q^2 \rangle$ [GeV ²]	0.0056
Maximum Current [μ A]	85
Target Length (cm)	150
ρ_{tgt} [g/cm ³] (T= 20K, P = 35 psia)	0.0715
Max. Luminosity [cm ⁻² sec ⁻¹]	$3.4 \cdot 10^{39}$
σ [μ Barn]	≈ 40
Møller Rate [GHz]	≈ 135
Statistical Width(2 kHz flip) [ppm/pair]	≈ 83
Target Raster Size [mm]	5 x 5
ΔA_{raw} [ppb]	≈ 0.6
Background Fraction	≈ 0.08
P_{beam}	$\approx 85\%$
$\langle A_{pv} \rangle$ [ppb]	≈ 35
$\Delta A_{stat} / \langle A_{expt} \rangle$	2.1%
$\delta(\sin^2 \theta_W)_{stat}$	0.00026

Table 1. Nominal design parameters for the proposed Moller measurement [MOLLER 2012].

The scope of this report is to estimate the effects of the pion detector shielding on the pion detector itself and on the surrounding detectors. Any desired or undesired effects are function of the background rates produced at the shielding. They are reported here as a function of shielding thickness. Studying the shielding properties as a separate problem reduces the amount of the simulation needed to optimize the whole Moller experiment. This report could be used as the initial step for the Moller experiment's pion detector design. Finally, parts of this report could be of help in the process designing other subparts of the Moller experiment or, generally, for other experiments using 12 GeV electron beam at Jefferson Lab.

Detectors overview, including pion detector shielding positioned in front of the pion detector, is shown in Figure 1.

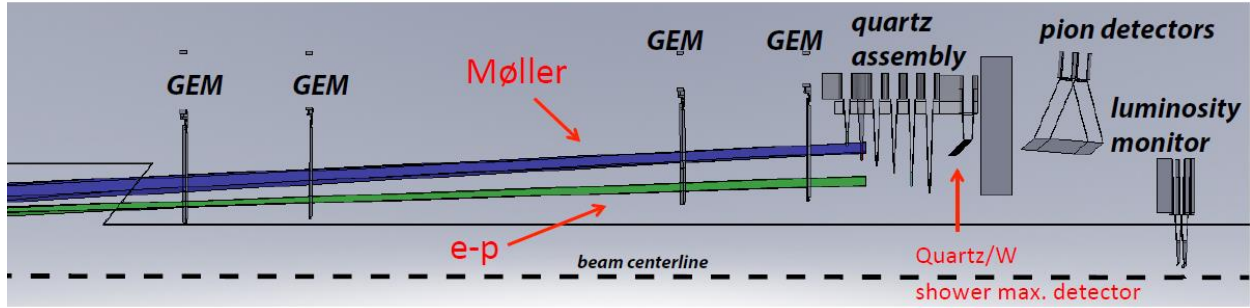


Figure 1. Schematics of the pion detectors shielding and the position of the surrounding detectors.

Propagation of particles through the shielding material, their range, the associate production of secondary particles and energy deposition was obtained using a simulation tool called FLUKA [FERRARI 2005, BATTISTONI 2007], a fully integrated particle physics Monte Carlo simulation package with many applications in high energy experimental physics and engineering, shielding, detectors and telescopes design, cosmic ray studies, dosimetry, medical physics and radio-biology. Once the incoming particles are generated and the properties of the material are known, it is straight forward to simulate the shielding capabilities. The physical mechanisms implemented in today's simulation software are very accurate and the differences between the simulated and measured results are in the most cases negligible.

In this report detailed study of the shielding properties are done for pion and electron energy of 1.8 GeV, the lowest energy in Table 1. Effects of the shielding are calculated for the lead shielding thicknesses of 20 and 50 cm.

II. Results for 20 cm thick lead shielding

In this section we study the effects of pions and electrons impinging on a 20 cm x 20 cm x 20 cm lead block. In addition to the total deposited energy in the block, the fluences of pions, muons, neutrons, protons, electrons, photons, lambdas and sigma- are also calculated in units of number of particles per cm^2 normalized to number of incoming particles per cm^2 . With such a choice of units one only needs to multiply shown fluences with primary particles rates (which can be calculated separately) to get the fluences expected in the Moller experiment. In the simulation the cutoff energy threshold for all the particles was 10^{-5} GeV, except for the neutrons where the cutoff threshold was 10^{-8} GeV.

In the case of the pions, the total deposited energy is shown in Figure 1 in units of MeV/cm^3 . The average deposited energy in the entire lead block was 718 MeV per incoming pion. The fluences integrated over all the secondary particles energies are shown in Figures 2-9 and Figures 10-17.

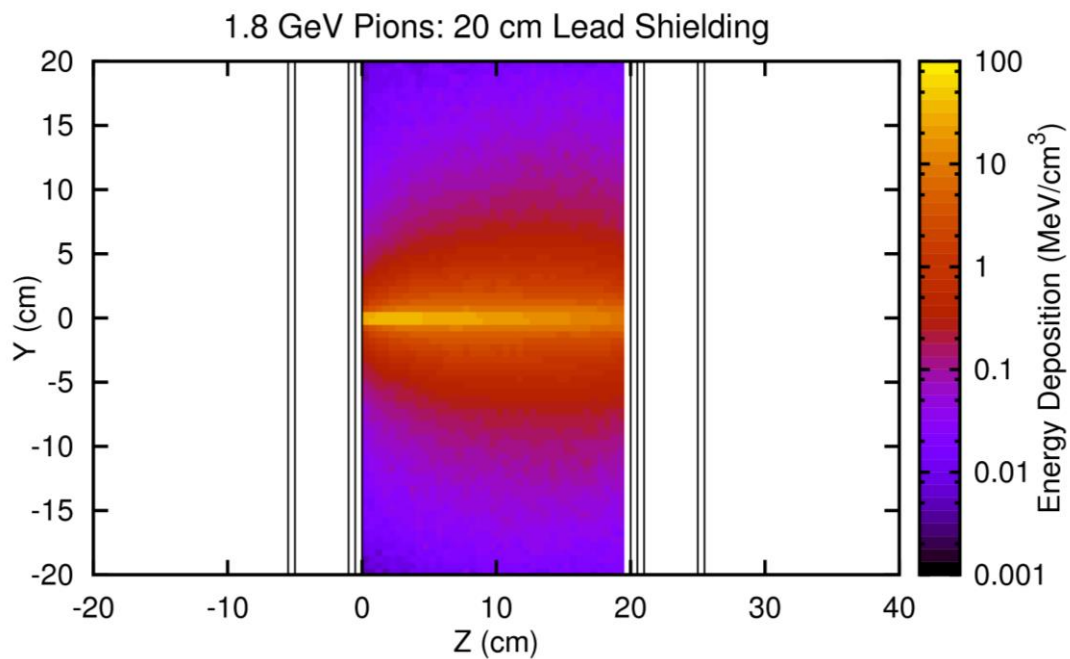


Figure 1. Total deposited energy in the 20 cm thick lead block per incoming 1.8 GeV pion.

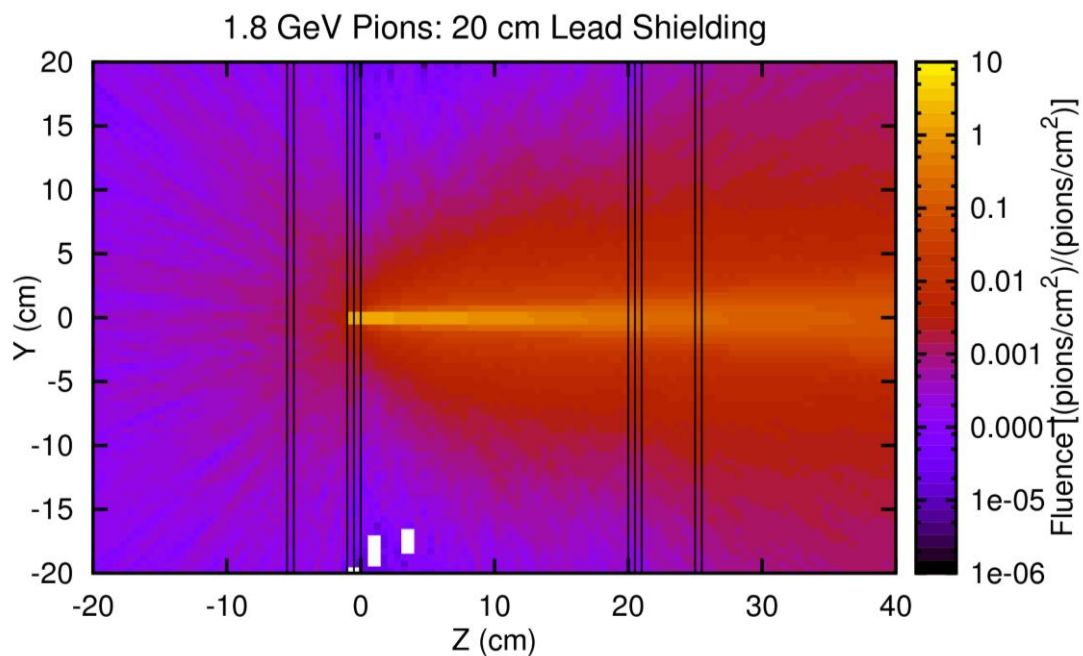


Figure 2. Pion fluence in the case of the 20 cm thick lead block per incoming 1.8 GeV pion.

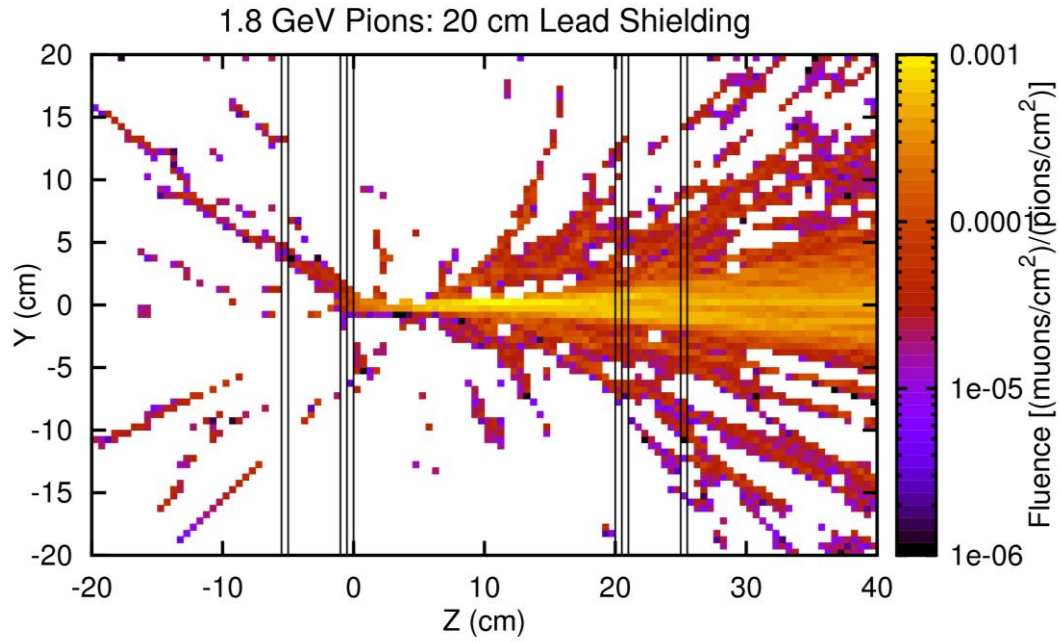


Figure 3. Muon fluence in the case of the 20 cm thick lead block per incoming 1.8 GeV pion.

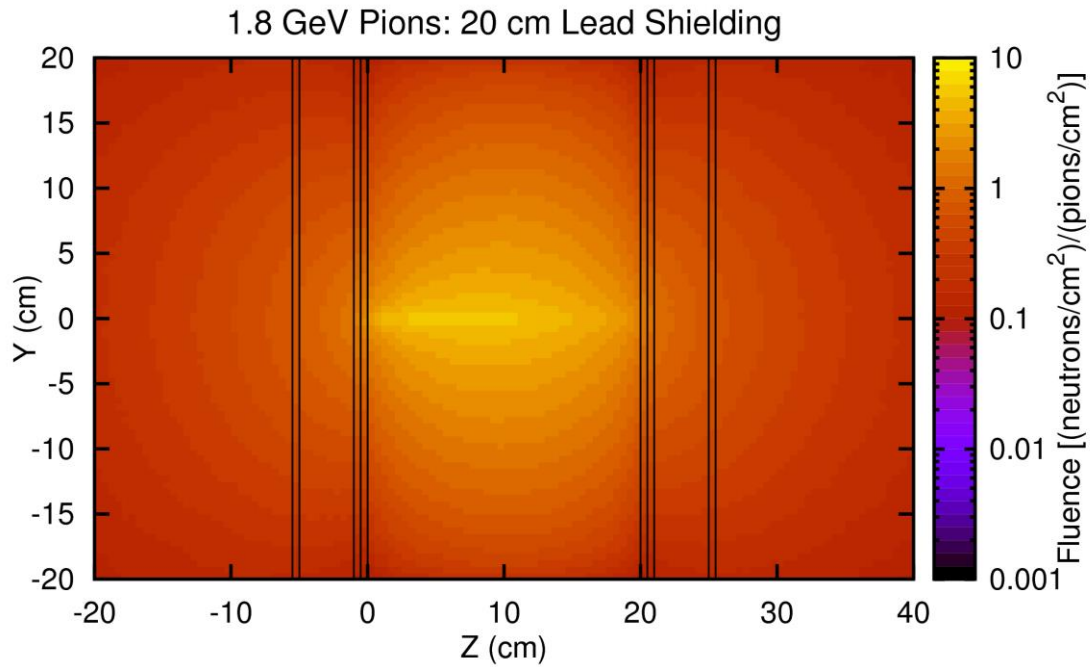


Figure 4. Neutron fluence in the case of the 20 cm thick lead block per incoming 1.8 GeV pion.

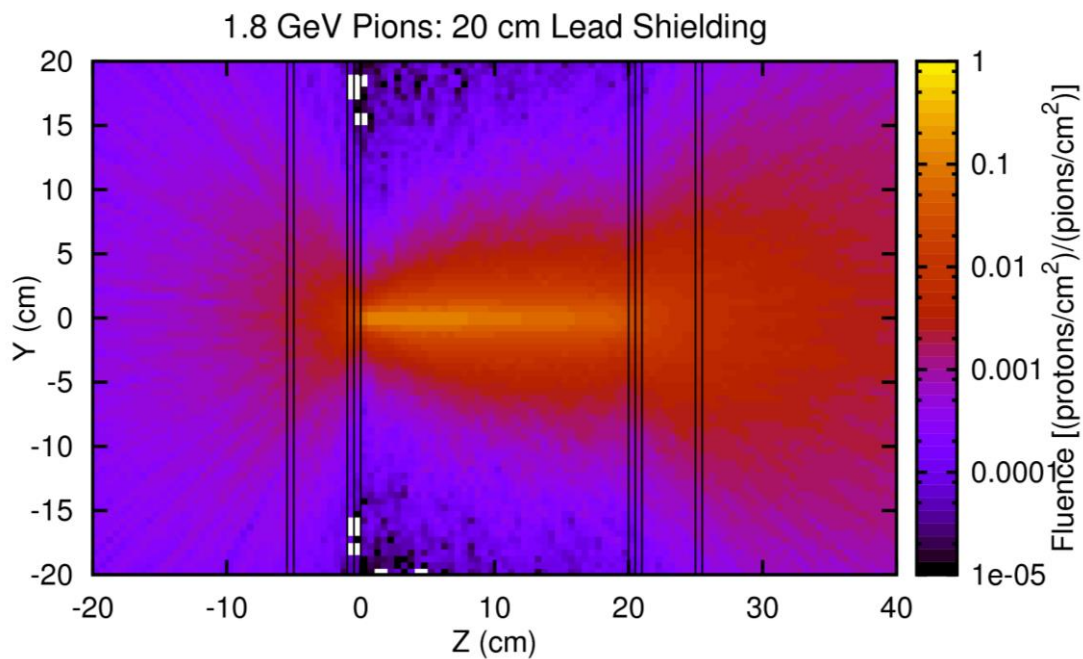


Figure 5. Proton fluence in the case of the 20 cm thick lead block per incoming 1.8 GeV pion.

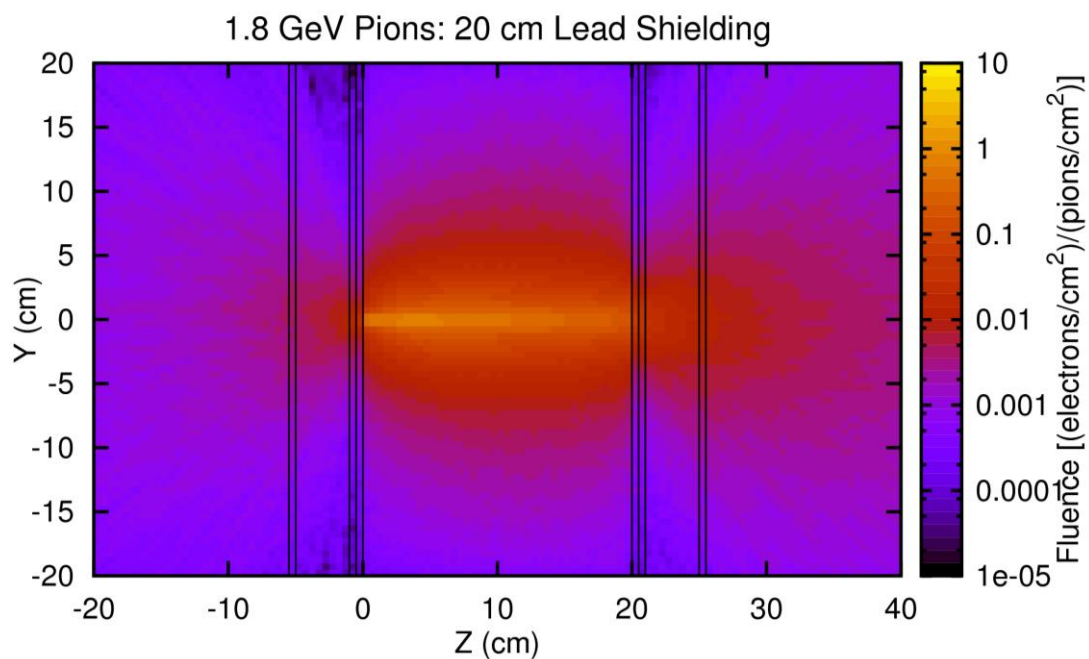


Figure 6. Electron fluence in the case of the 20 cm thick lead block per incoming 1.8 GeV pion.

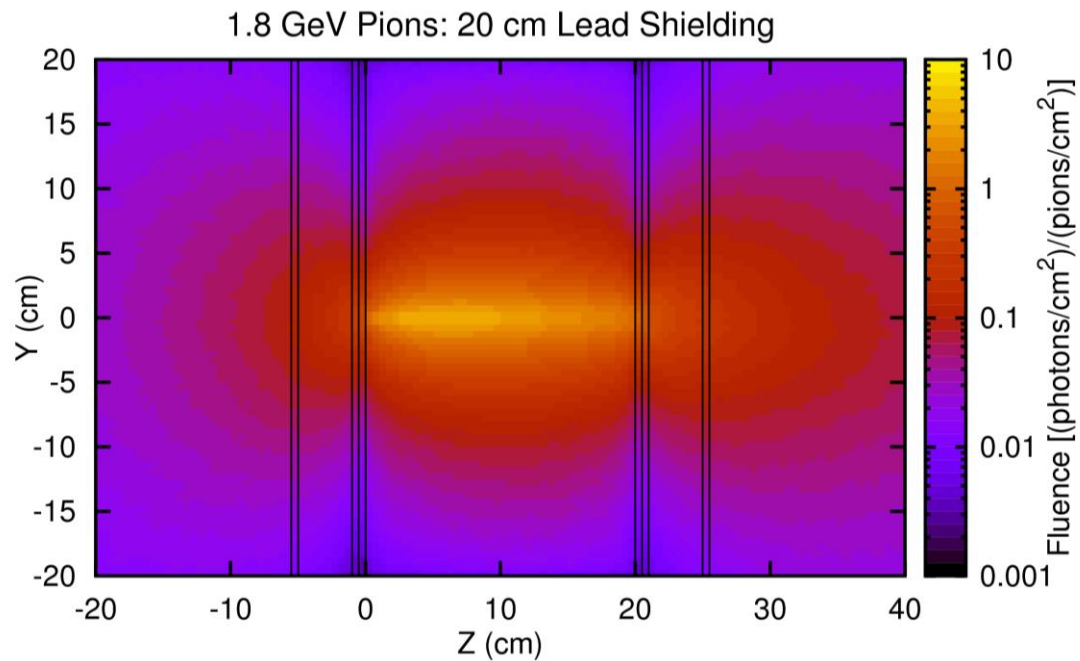


Figure 7. Photon fluence in the case of the 20 cm thick lead block per incoming 1.8 GeV pion.

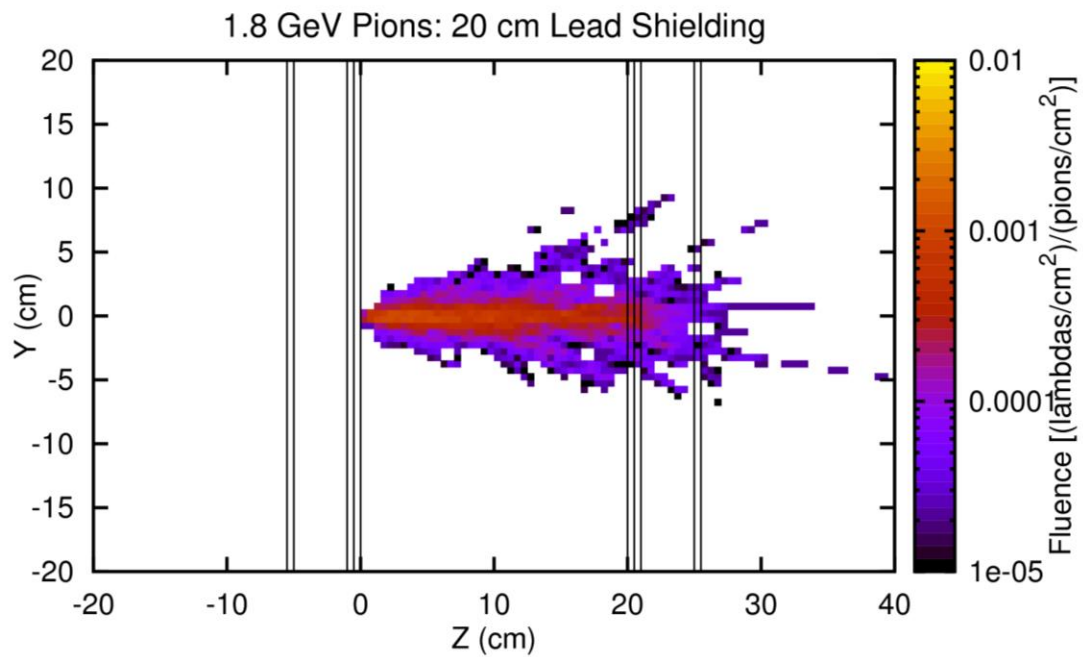


Figure 8. Lambda fluence in the case of the 20 cm thick lead block per incoming 1.8 GeV pion.

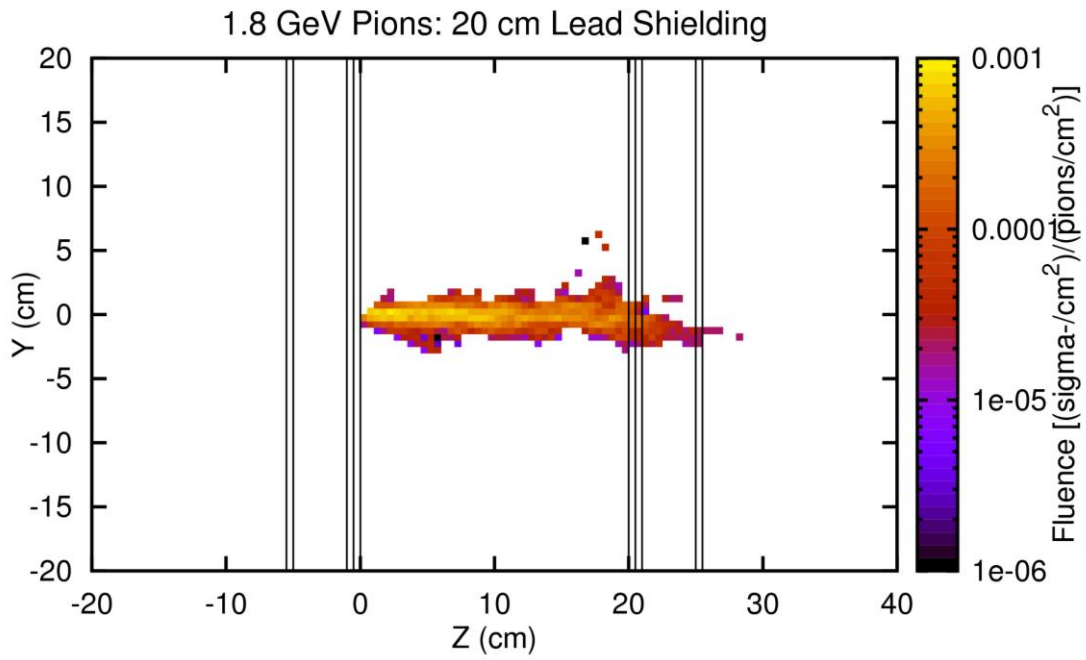


Figure 9. Sigma- fluence in the case of the 20 cm thick lead block per incoming 1.8 GeV pion.

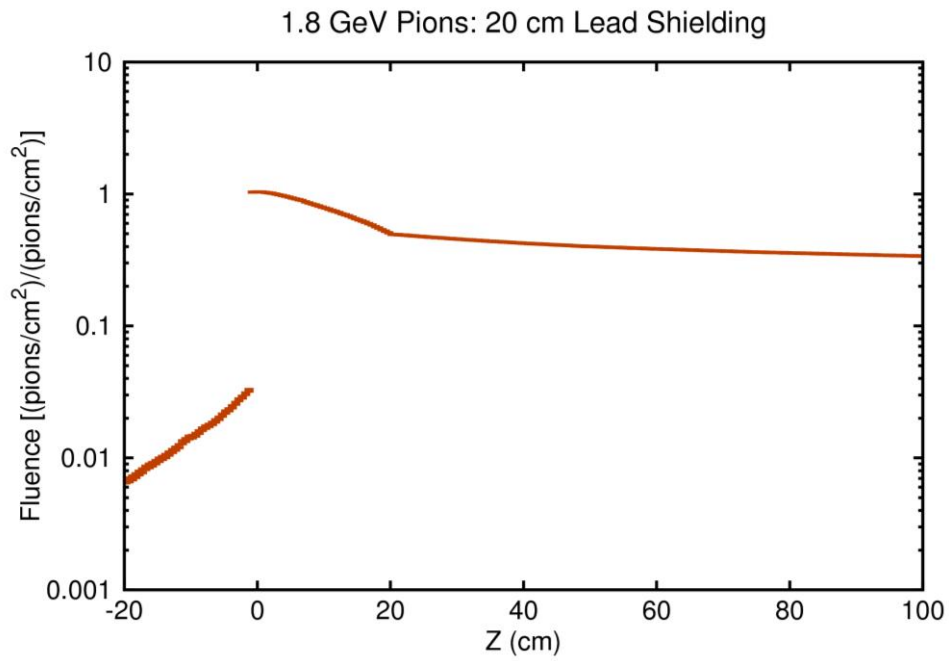


Figure 10. Energy integrated pion fluence as a function of position.

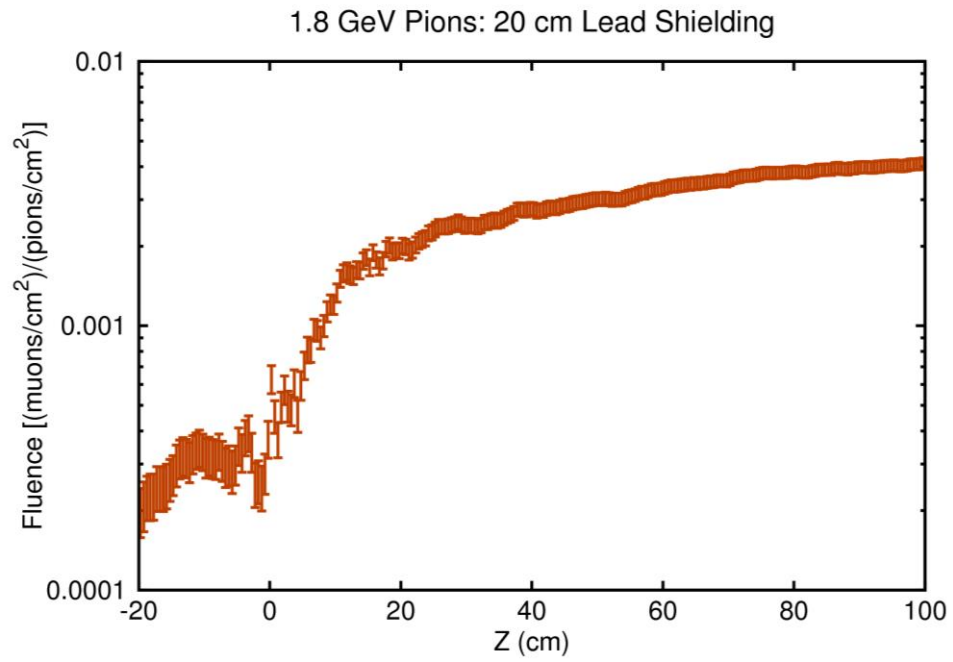


Figure 11. Energy integrated muon fluence as a function of position.

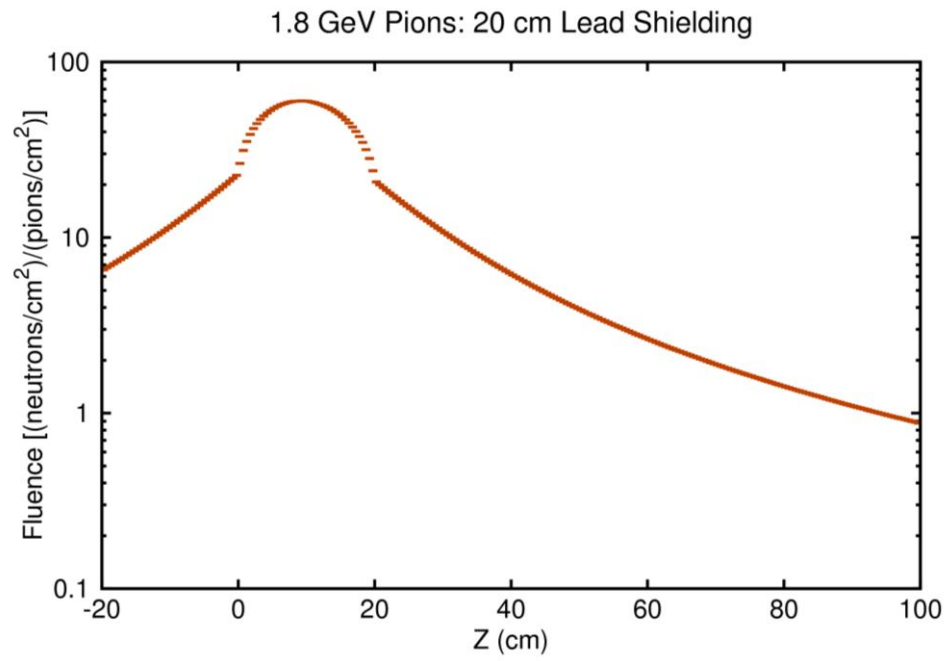


Figure 12. Energy integrated neutron fluence as a function of position.

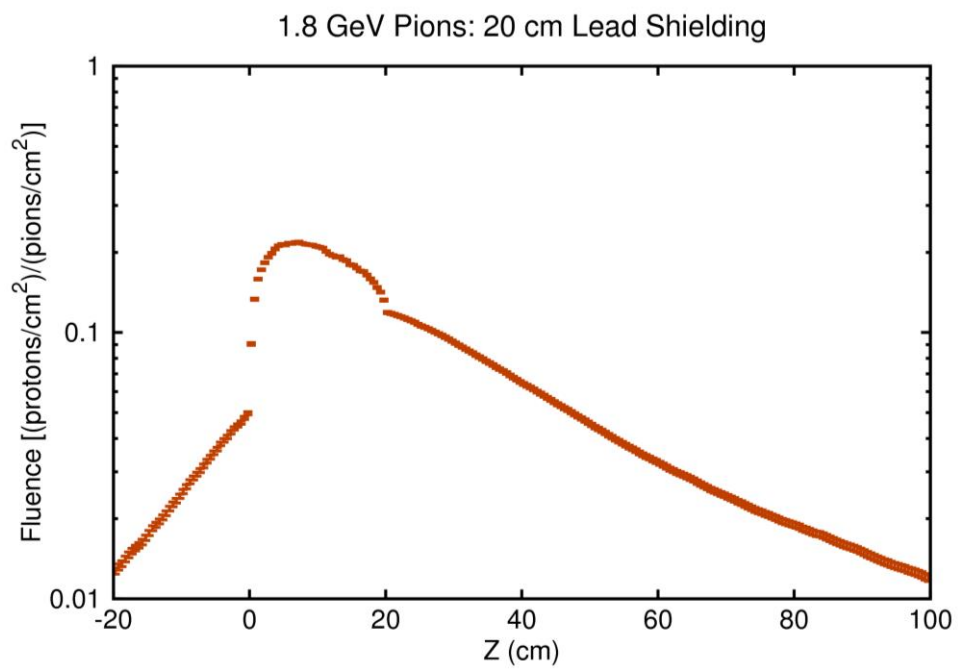


Figure 13. Energy integrated proton fluence as a function of position.

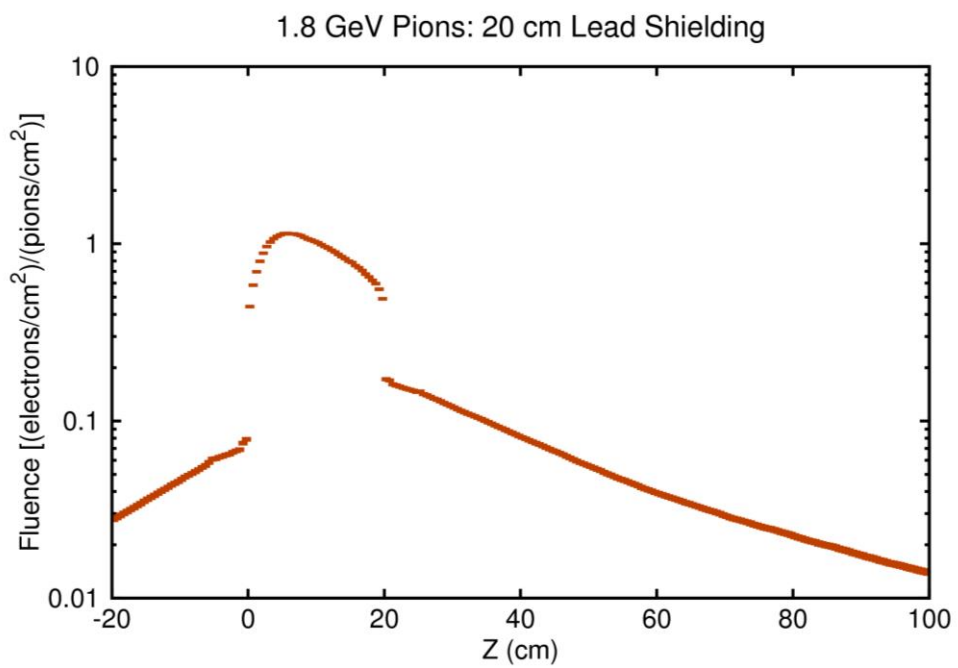


Figure 14. Energy integrated electron fluence as a function of position.

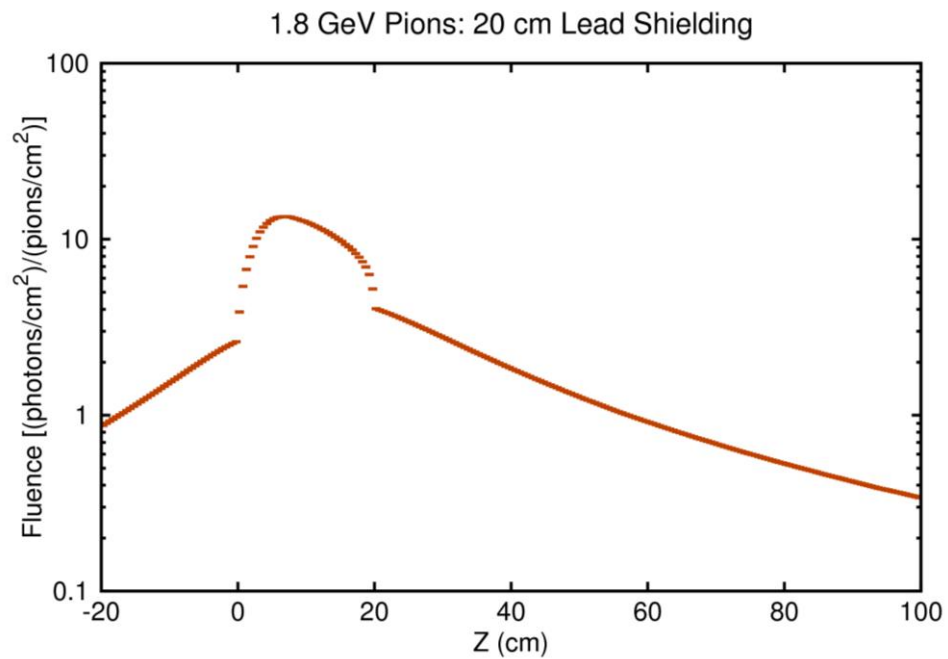


Figure 15. Energy integrated photon fluence as a function of position.

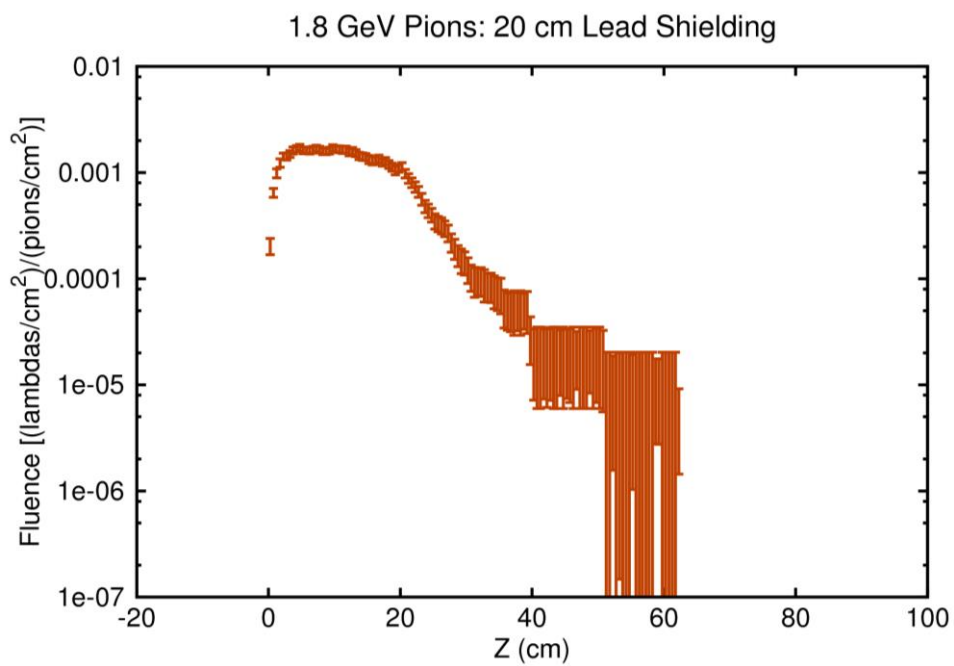


Figure 16. Energy integrated lambda fluence as a function of position.

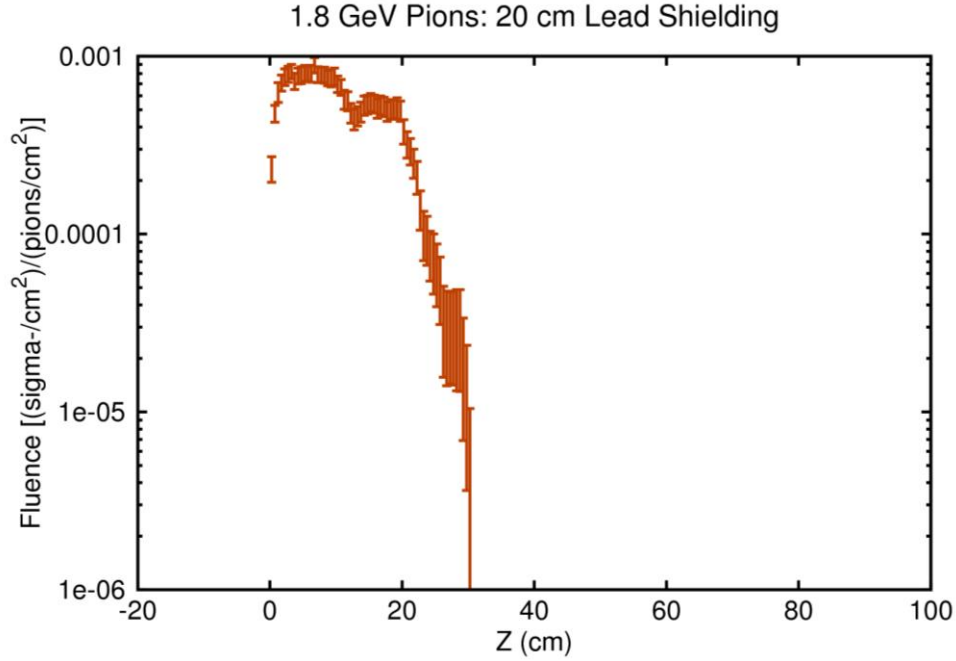


Figure 17. Energy integrated sigma- fluence as a function of position.

The fluences shown in Figures 10-17 are integrated over all the secondary particles energies and can be used to calculate the background rates, but, to fully understand the background, it is also important to know the secondary particles energy spectra. In Figures 18-25 the isoethargic spectra are shown for the secondary particles produced by the shielding in forward and backward directions. The reason for using isoethargic spectra is that the dynamic range of the energies of the secondary particles requires a logarithmic energy scale. For such a scale the area under the isoethargic spectrum curve is proportional to the number of particles in a particular energy interval.

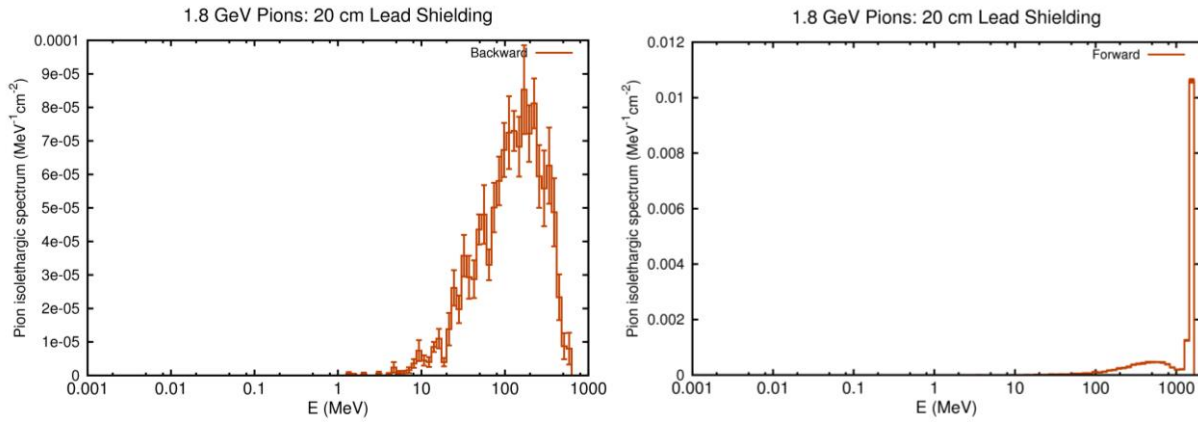


Figure 18. Pion isoethargic spectrum for backward and forward produced pions in a 20 cm thick lead shielding.

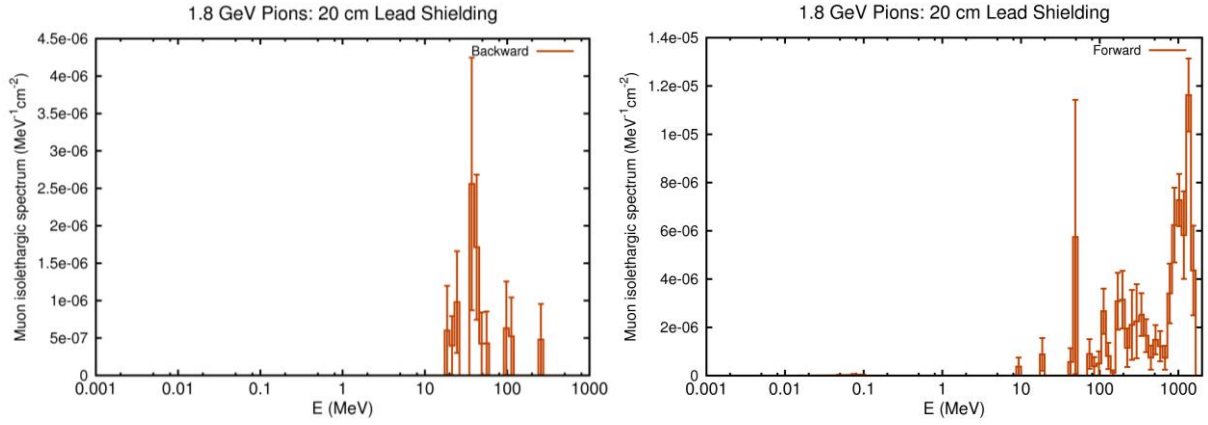


Figure 19. Muon isolethargic spectrum for backward and forward produced muons in a 20 cm thick lead shielding.

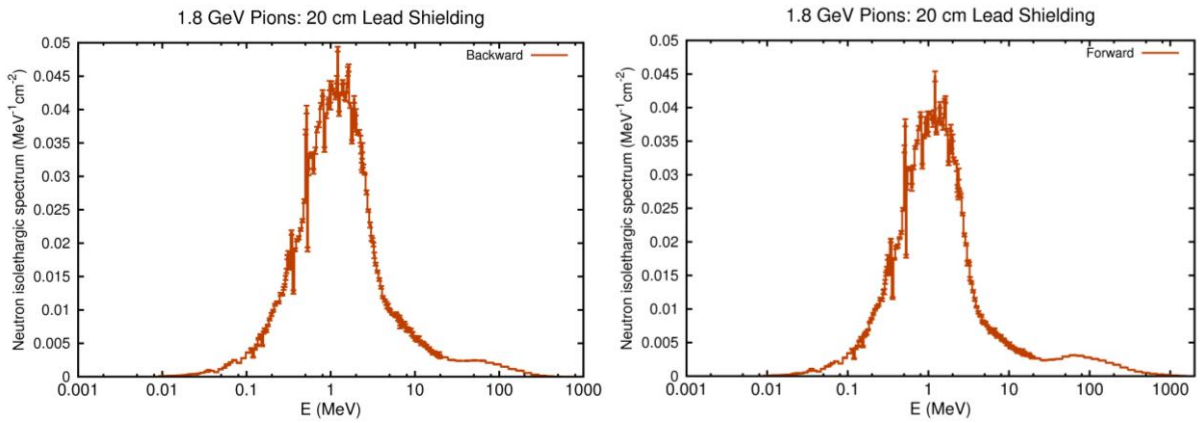


Figure 20. Neutron isolethargic spectrum for backward and forward produced neutrons in a 20 cm thick lead shielding.

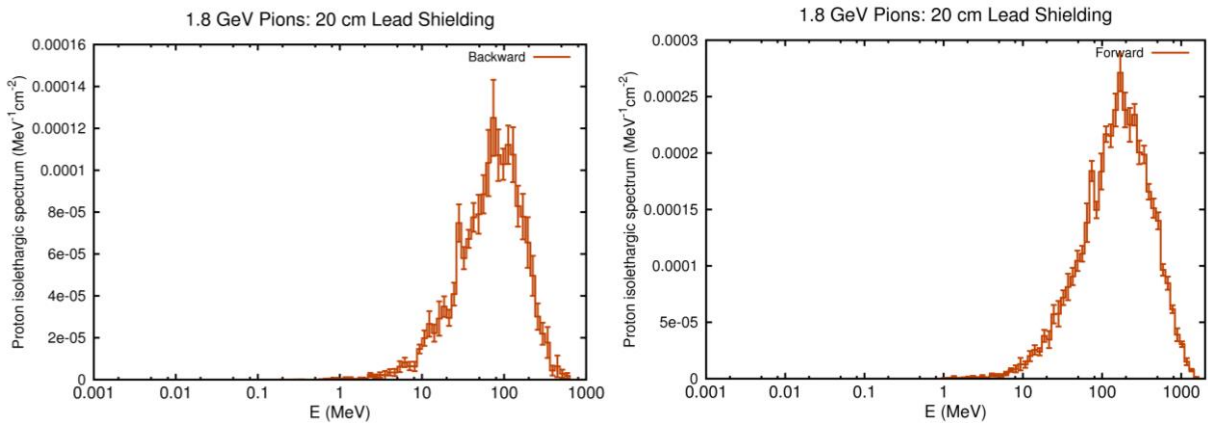


Figure 21. Proton isolethargic spectrum for backward and forward produced protons in a 20 cm thick lead shielding.

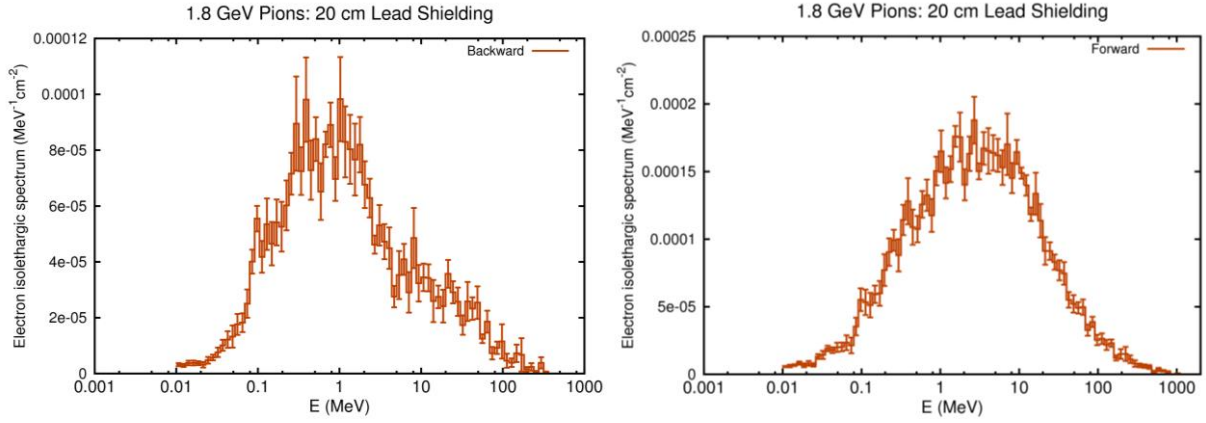


Figure 22. Electron islethargic spectrum for backward and forward produced electrons in a 20 cm thick lead shielding.

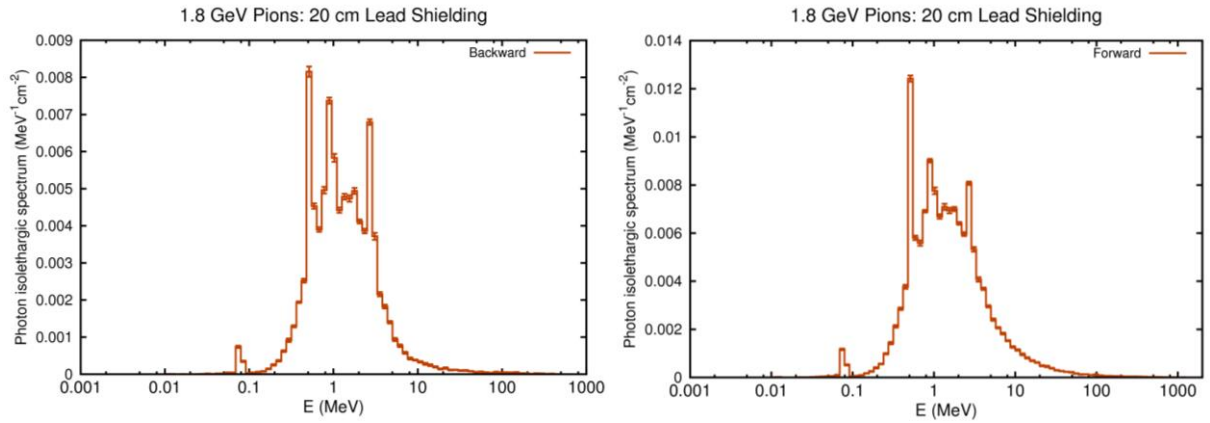


Figure 23. Photon islethargic spectrum for backward and forward produced photons in a 20 cm thick lead shielding.

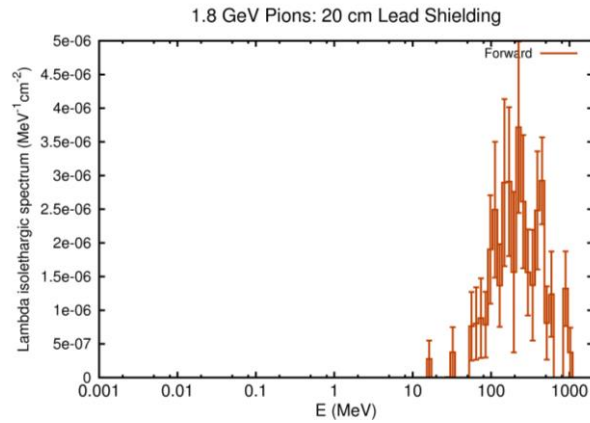


Figure 24. Lambda islethargic spectrum for backward and forward produced lambdas in a 20 cm thick lead shielding.

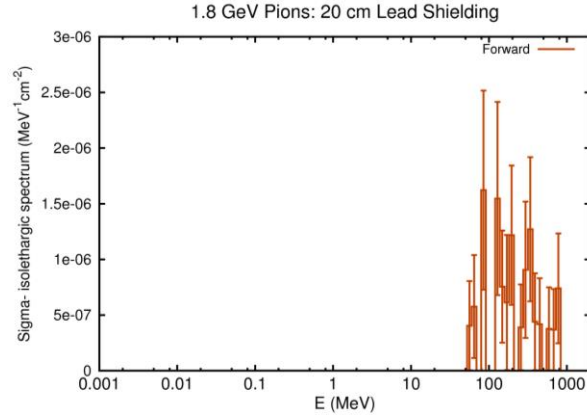


Figure 25. Sigma- isolethargic spectrum for backward and forward produced sigma- in a 20 cm thick lead shielding.

In the case of the electrons, the total deposited energy is shown in Figure 26 in units of MeV/cm^3 . The average deposited energy in the entire lead block was 1786 MeV per incoming electron. The fluences integrated over all secondary particles energies are shown in Figures 27-31 and Figures 32-36.

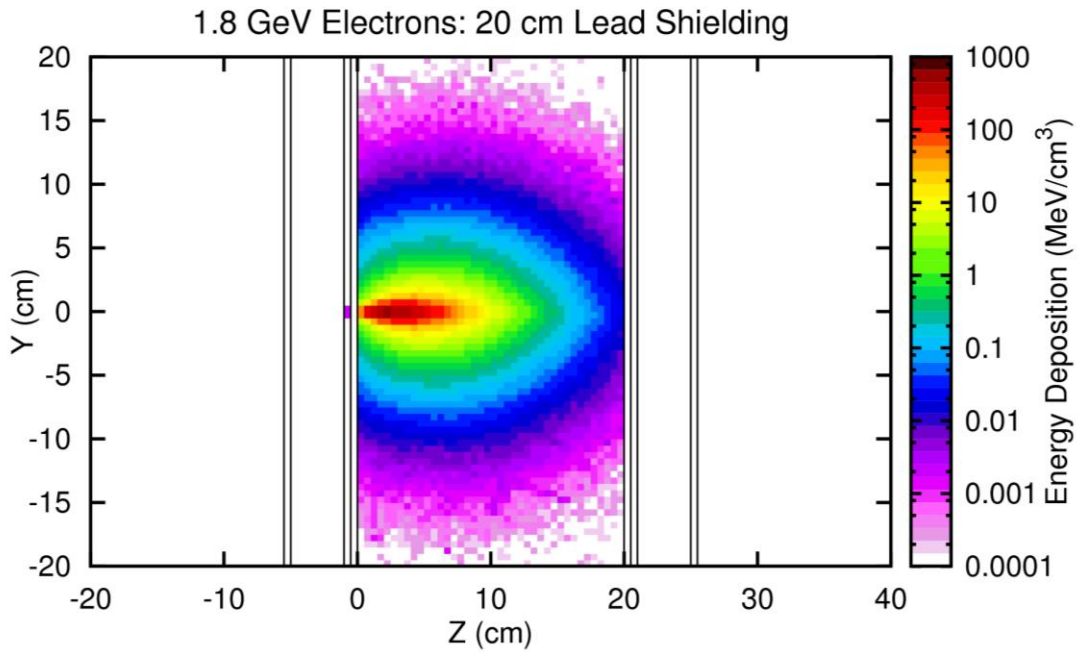


Figure 26. Total deposited energy in the 20 cm thick lead block per incoming 1.8 GeV electron.

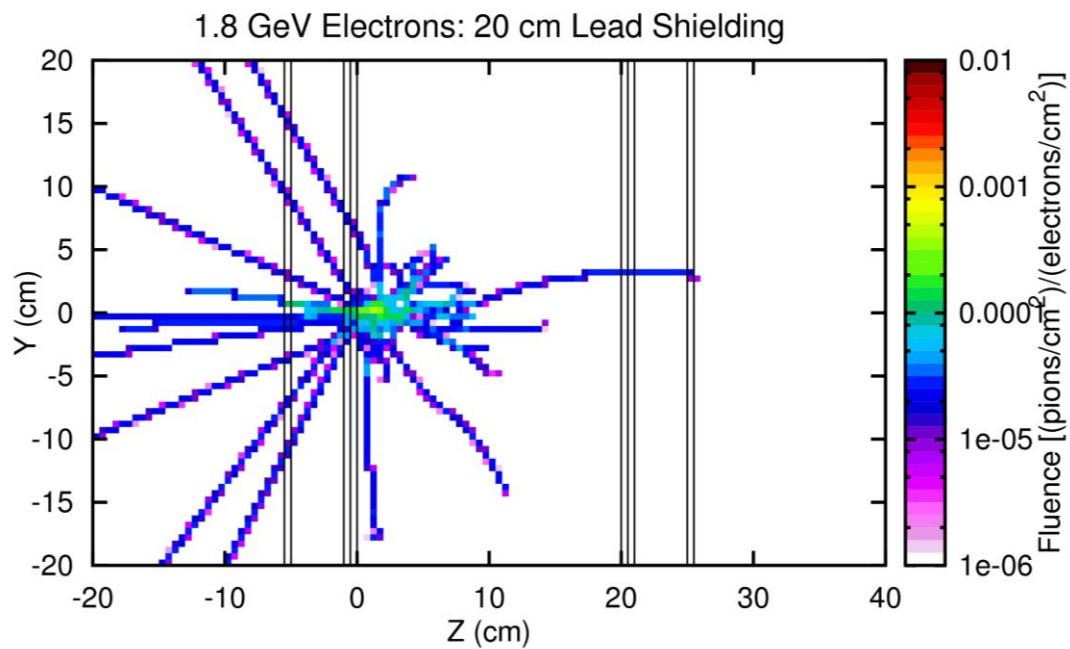


Figure 27. Pion fluence in the case of the 20 cm thick lead block per incoming 1.8 GeV electron.

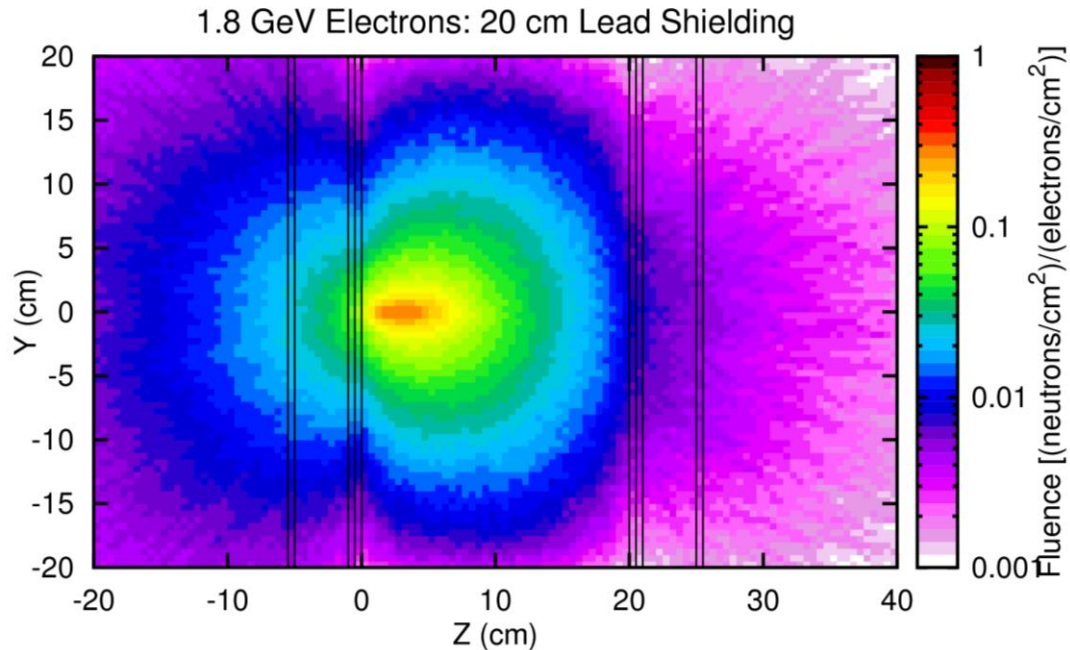


Figure 28. Neutron fluence in the case of the 20 cm thick lead block per incoming 1.8 GeV electron.

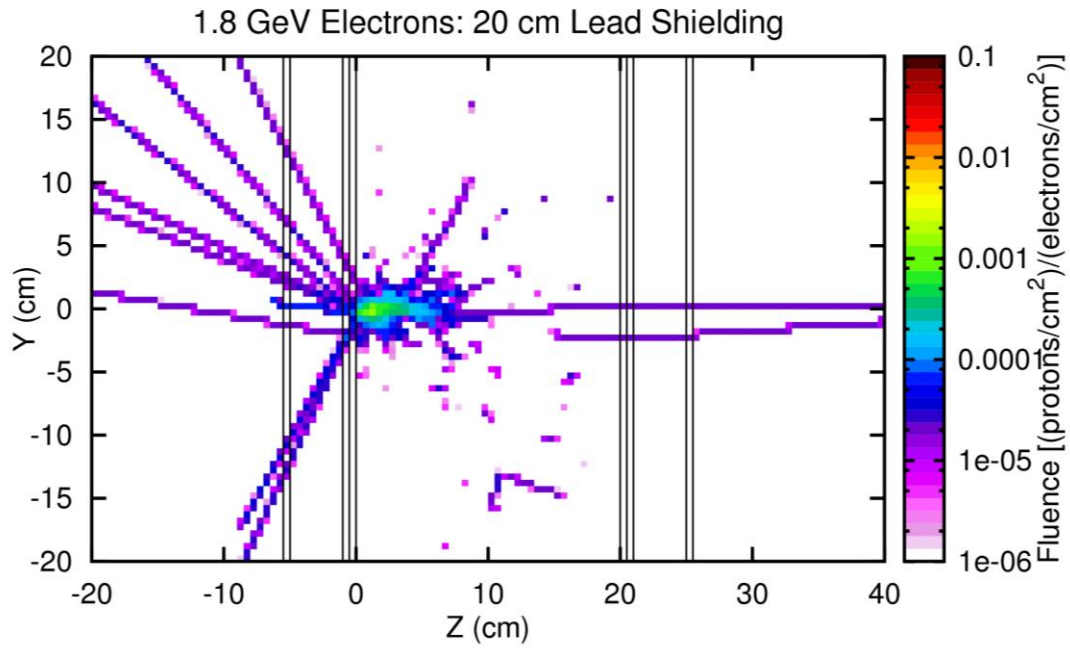


Figure 29. Proton fluence in the case of the 20 cm thick lead block per incoming 1.8 GeV electron.

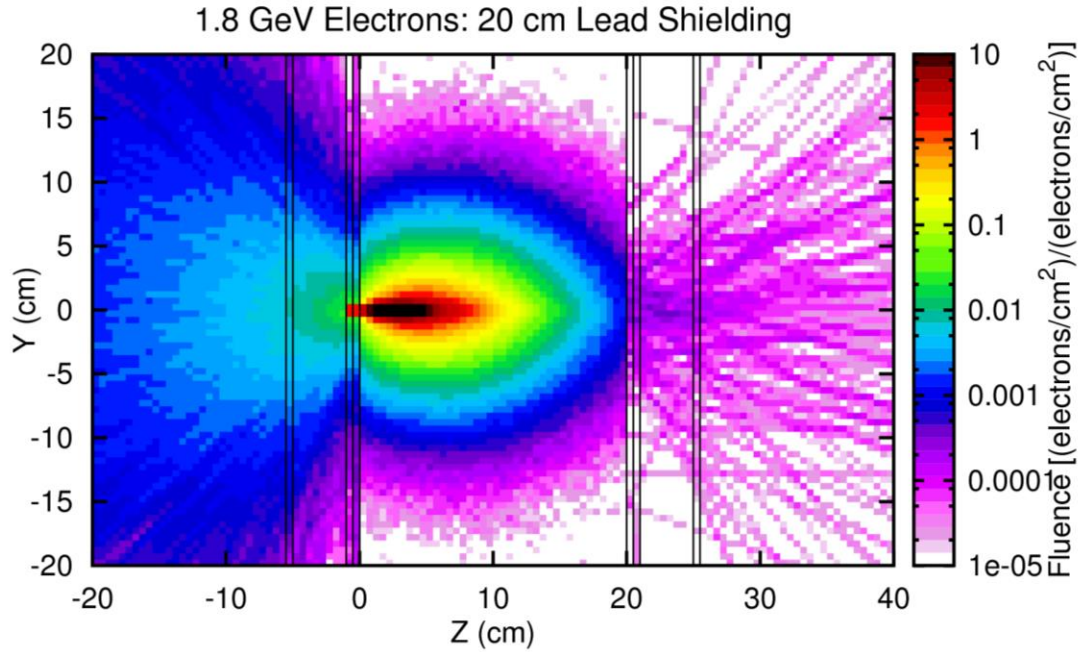


Figure 30. Electron fluence in the case of the 20 cm thick lead block per incoming 1.8 GeV electron.

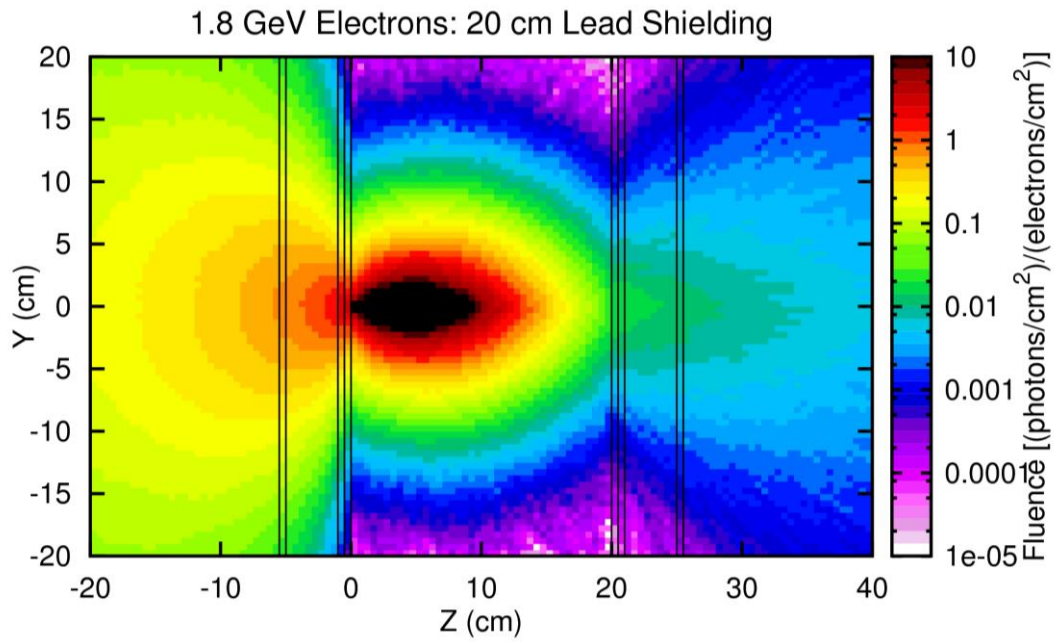


Figure 31. Photon fluence in the case of the 20 cm thick lead block per incoming 1.8 GeV electron.

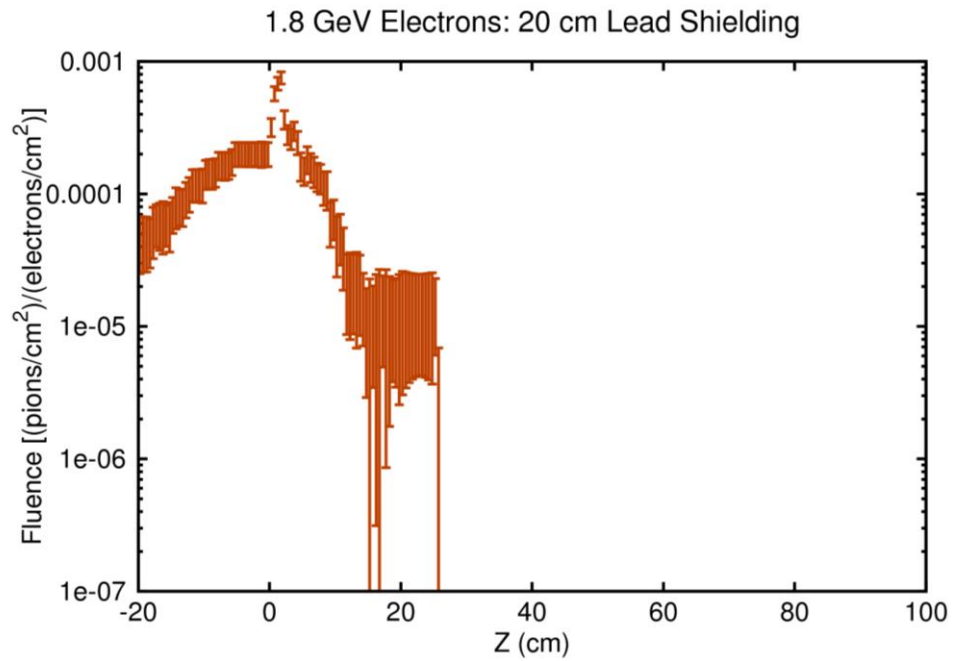


Figure 32. Energy integrated pion fluence as a function of position.

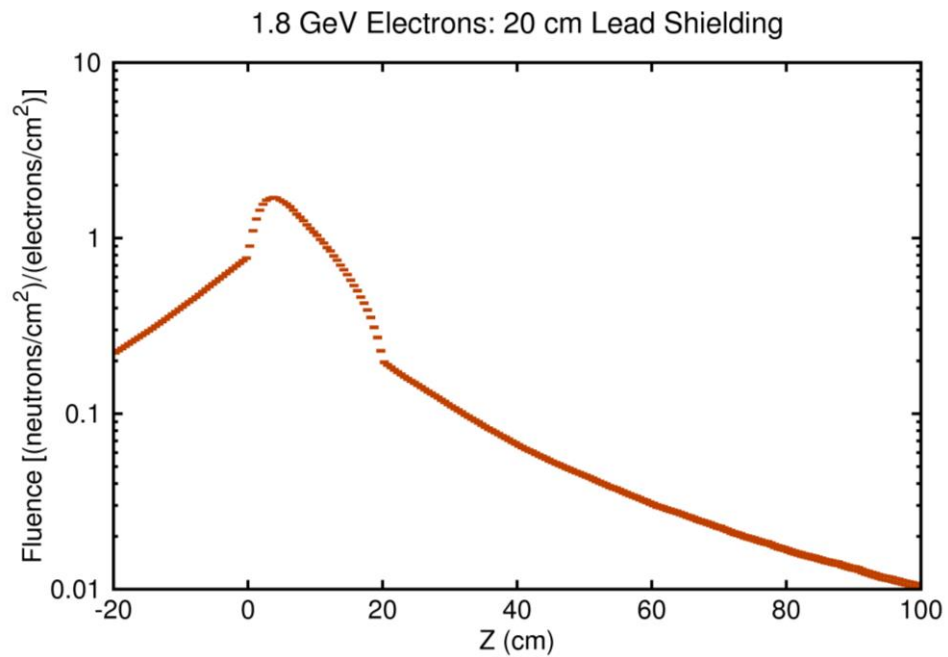


Figure 33. Energy integrated neutron fluence as a function of position.

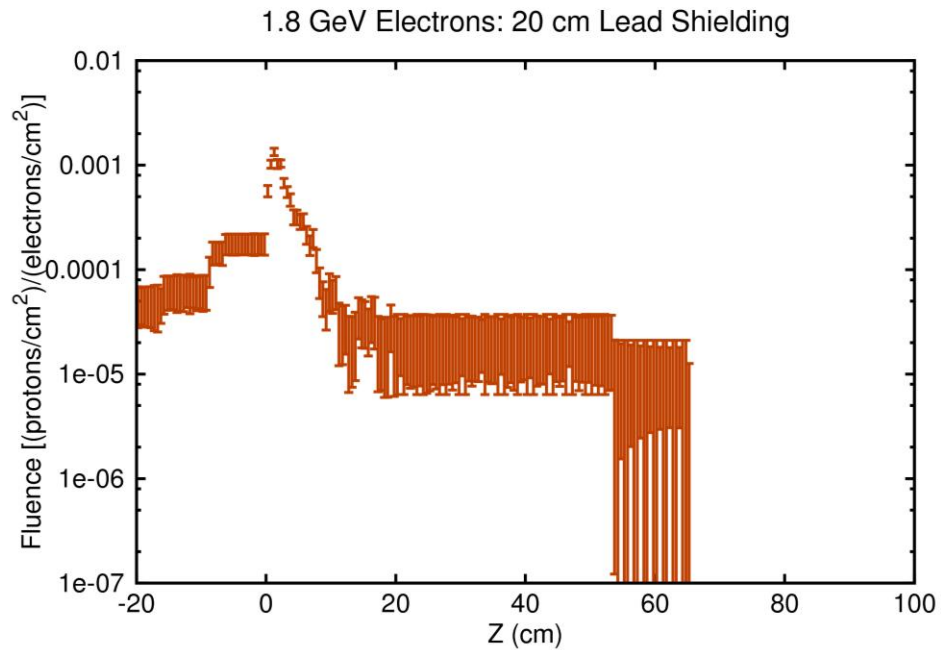


Figure 34. Energy integrated proton fluence as a function of position.

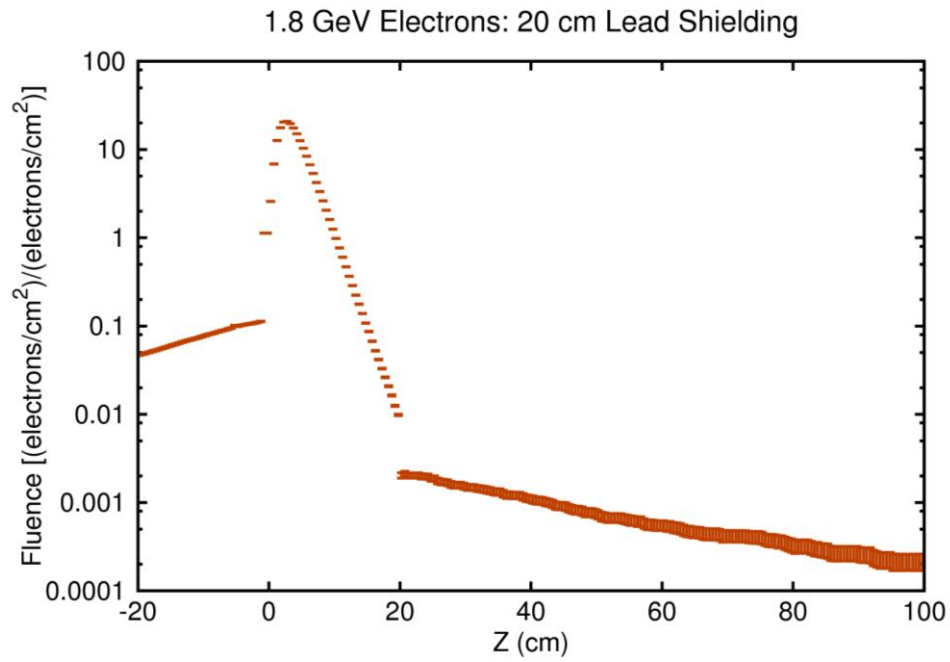


Figure 35. Energy integrated electron fluence as a function of position.

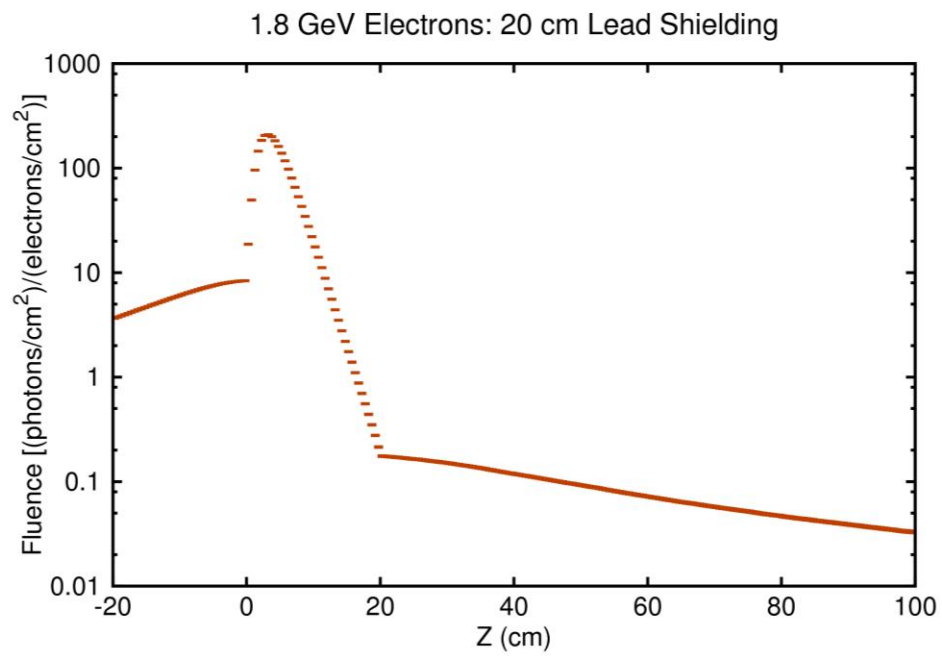


Figure 36. Energy integrated photon fluence as a function of position.

The fluences shown in Figures 27-36 are integrated over all the secondary particles energies and can be used to calculate the background rates, but, to fully understand the background, it is also important to know the secondary particles energy spectra. In Figures 37-41 the isoethargic spectra are shown for the secondary particles produced by the shielding in forward and backward directions. The reason for using isoethargic spectra is that the dynamic range of the energies of the secondary particles requires a logarithmic energy scale. For such a scale the area under the isoethargic spectrum curve is proportional to number of particles in a particular energy interval.

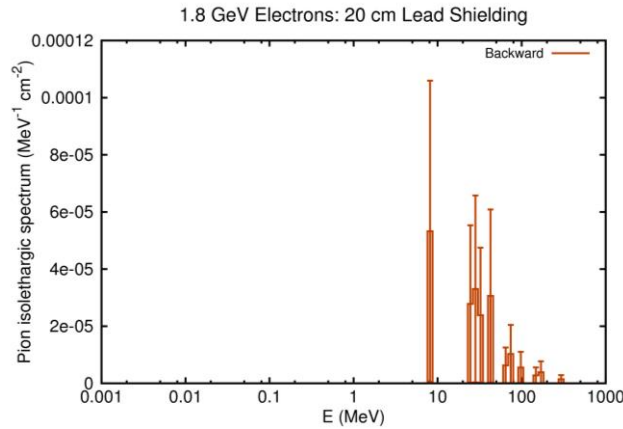


Figure 37. Pion isoethargic spectrum for backward produced pions in a 20 cm thick lead shielding.

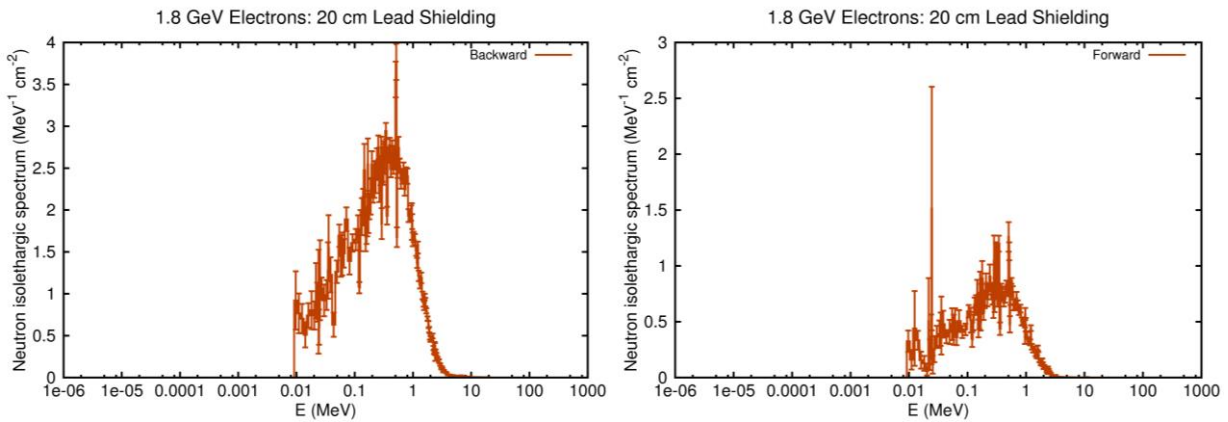


Figure 38. Neutron isoethargic spectrum for backward and forward produced neutrons in a 20 cm thick lead shielding.

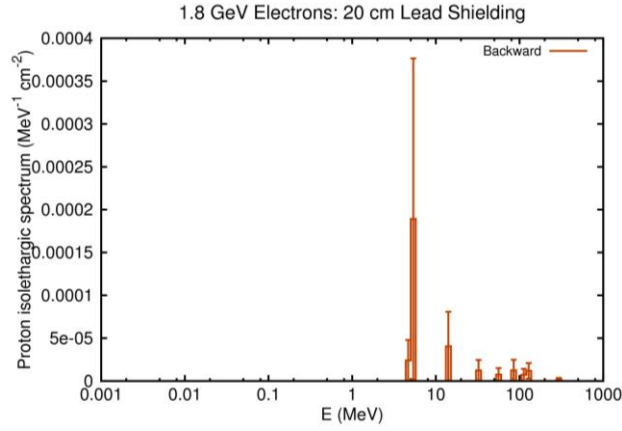


Figure 39. Proton isolethargic spectrum for backward produced protons in a 20 cm thick lead shielding.

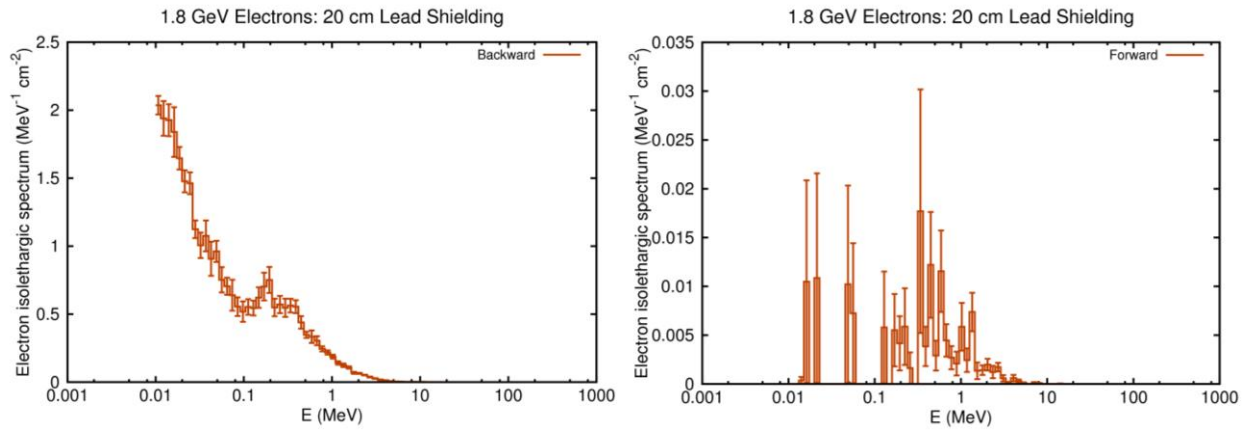


Figure 40. Electron isolethargic spectrum for backward and forward produced electrons in a 20 cm thick lead shielding.

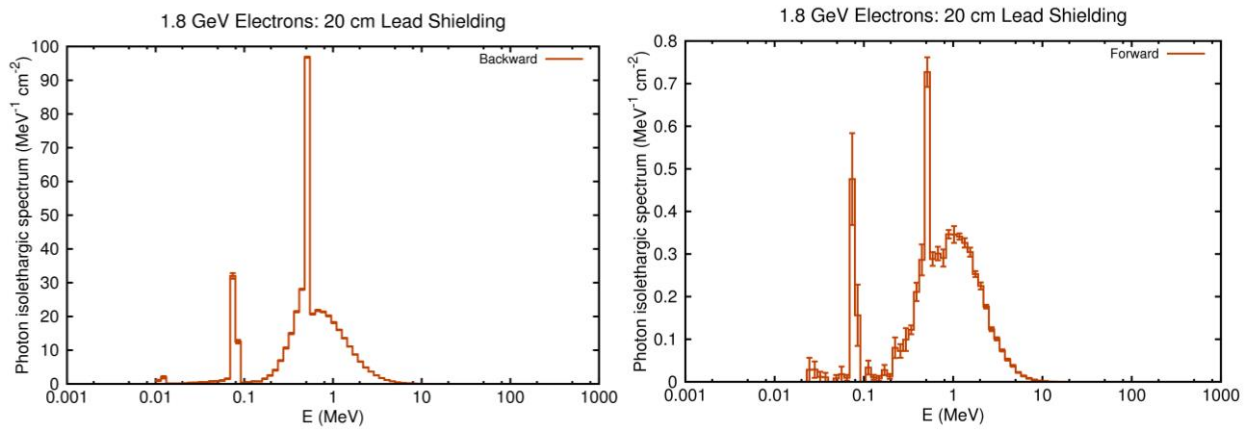


Figure 41. Photon isolethargic spectrum for backward and forward produced photons in a 20 cm thick lead shielding.

III Results for 50 cm thick lead shielding

In this section we study the effects of pions and electrons impinging on a 20 cm x 20 cm x 50 cm lead block. In addition to the total deposited energy in the block, the fluences of pions, muons, neutrons, protons, electrons, photons, lambdas and sigma- are also calculated in units of number of particles per cm^2 normalized to number of incoming particles per cm^2 . With such a choice of units one only needs to multiply shown fluences with primary particles rates (which can be calculated separately) to get the fluences expected in the Moller experiment. In the simulation the cutoff energy threshold for all the particles was 10^{-5} GeV, except for the neutrons where the cutoff threshold was 10^{-8} GeV.

In the case of the pions, the total deposited energy is shown in Figure 42 in units of MeV/cm^3 . The average deposited energy in the entire lead block was 1110 MeV per incoming pion. The fluences integrated over all secondary particles energies are shown in Figures 43-50 and Figures 51-58.

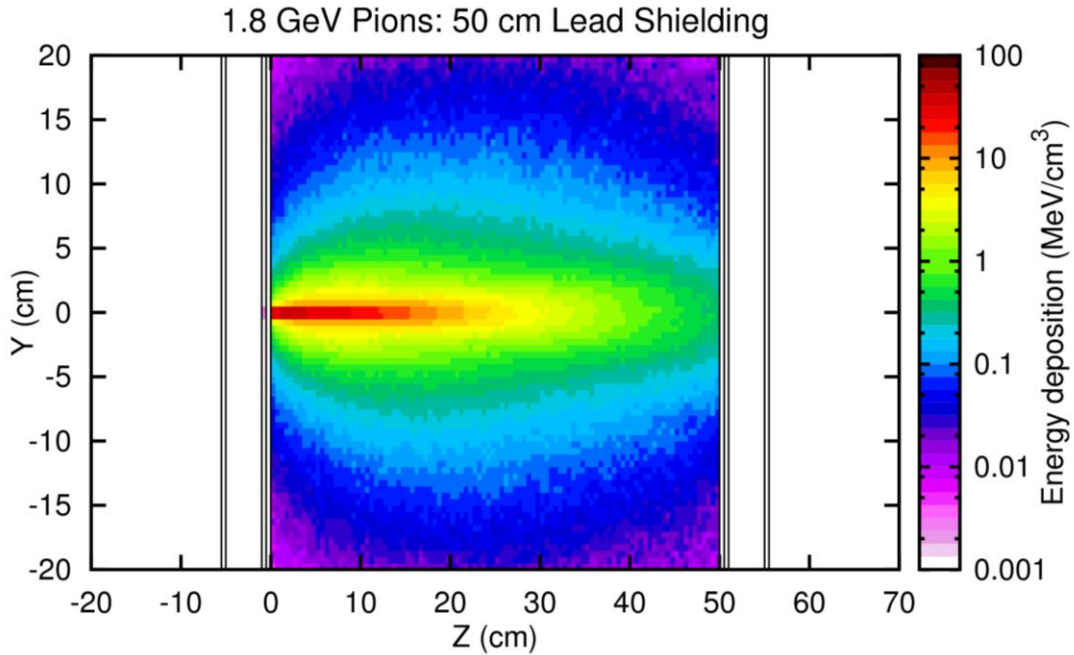


Figure 42. Total deposited energy in the 50 cm thick lead block per incoming 1.8 GeV pion.

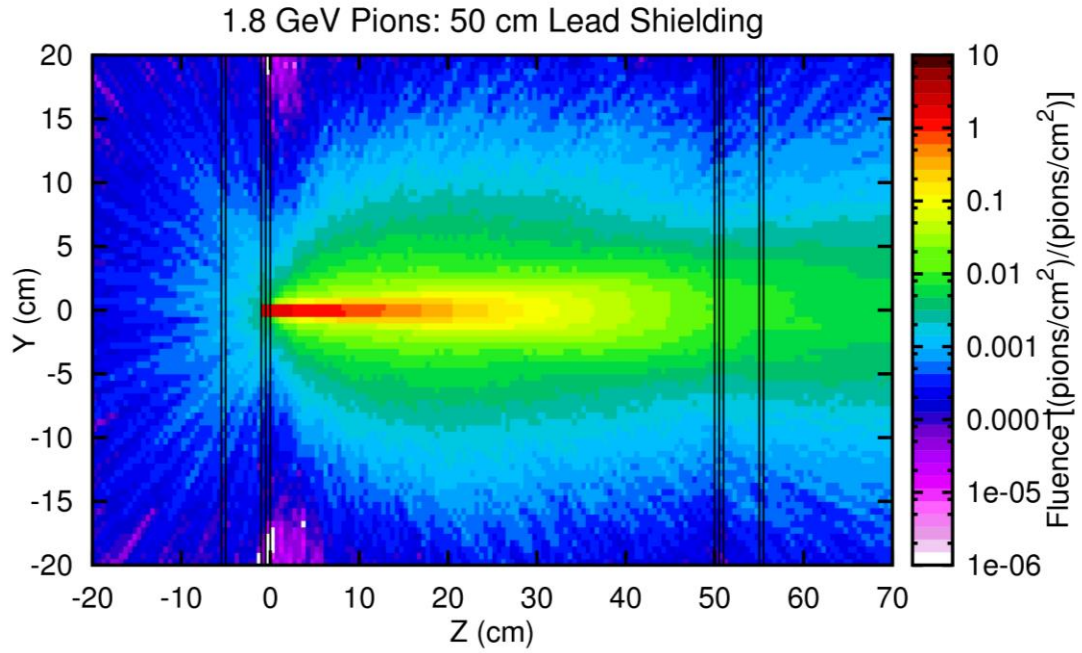


Figure 43. Pion fluence in the case of the 50 cm thick lead block per incoming 1.8 GeV pion.

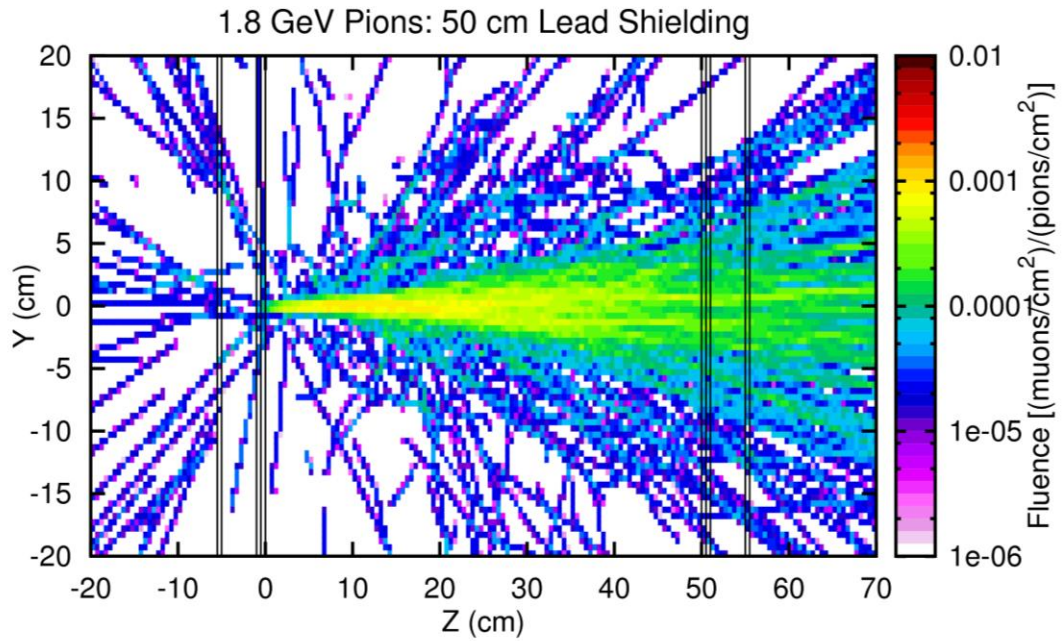


Figure 44. Muon fluence in the case of the 50 cm thick lead block per incoming 1.8 GeV pion.

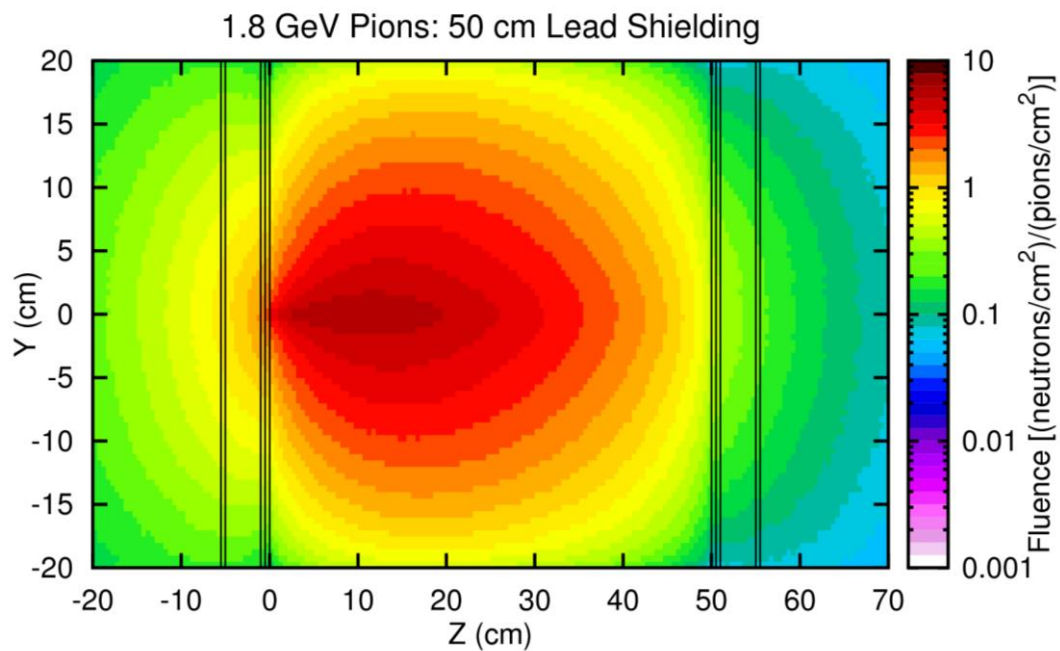


Figure 45. Neutron fluence in the case of the 50 cm thick lead block per incoming 1.8 GeV pion.

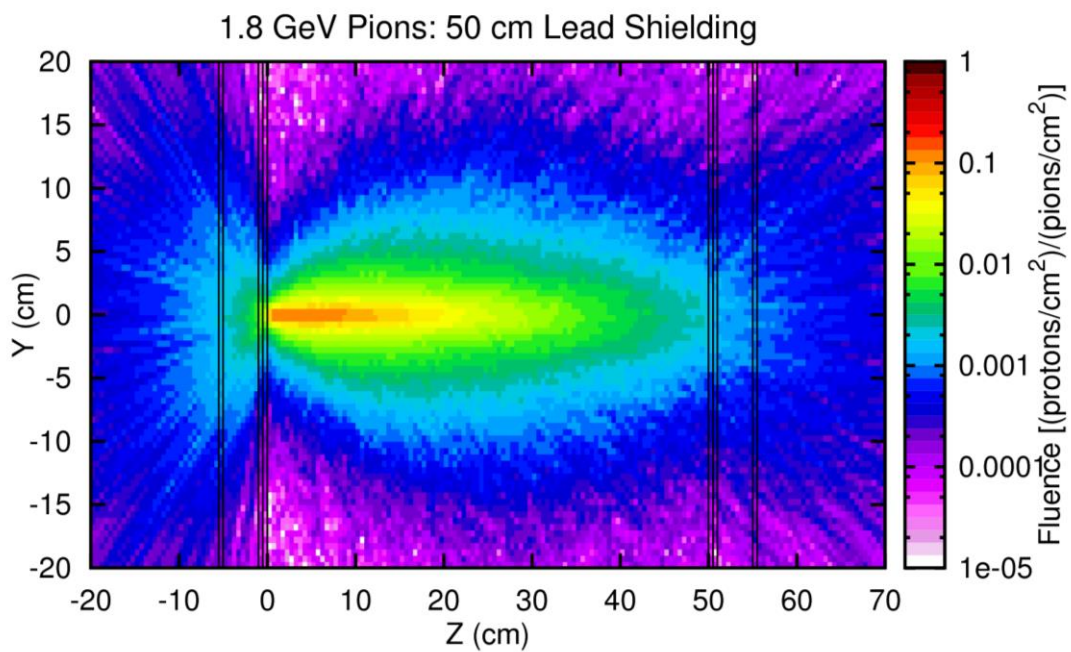


Figure 46. Proton fluence in the case of the 50 cm thick lead block per incoming 1.8 GeV pion.

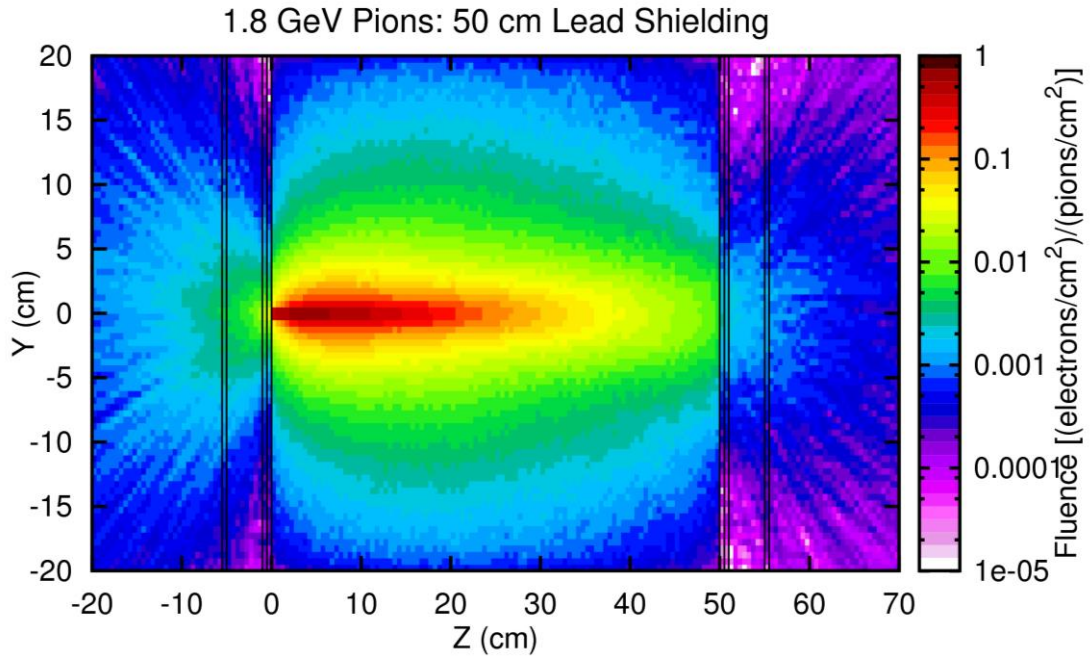


Figure 47. Electron fluence in the case of the 50 cm thick lead block per incoming 1.8 GeV pion.

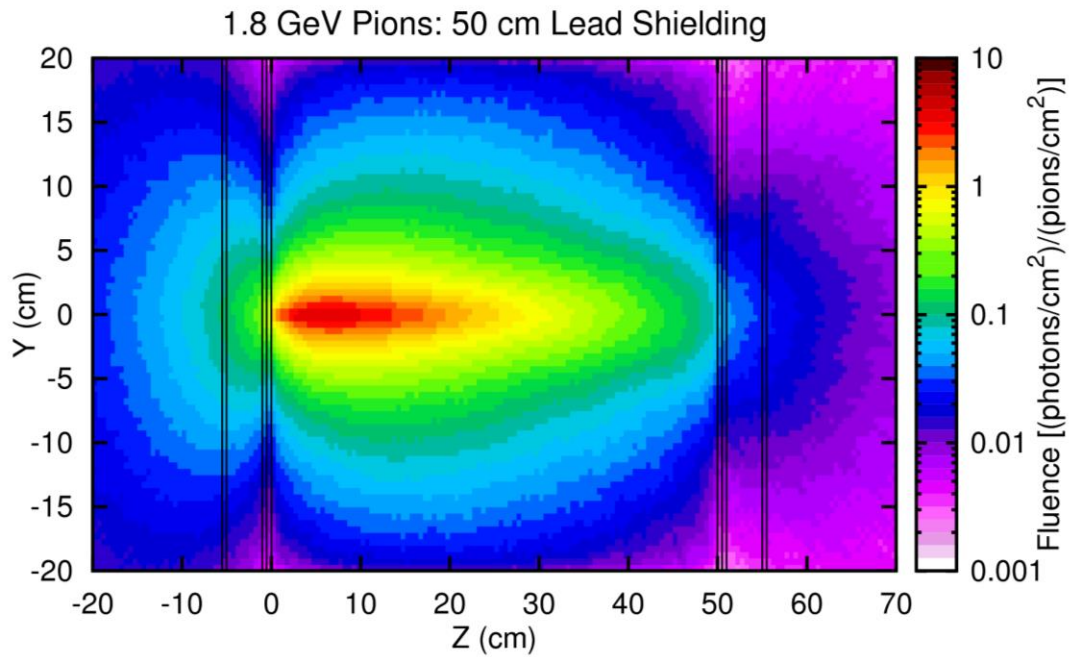


Figure 48. Photon fluence in the case of the 50 cm thick lead block per incoming 1.8 GeV pion.

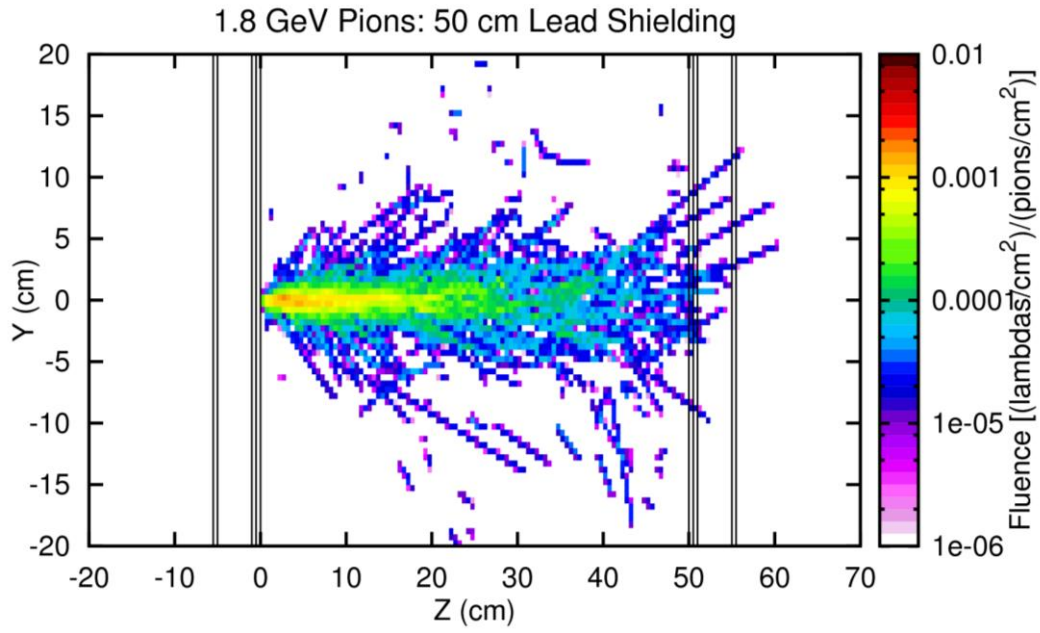


Figure 49. Lambda fluence in the case of the 50 cm thick lead block per incoming 1.8 GeV pion.

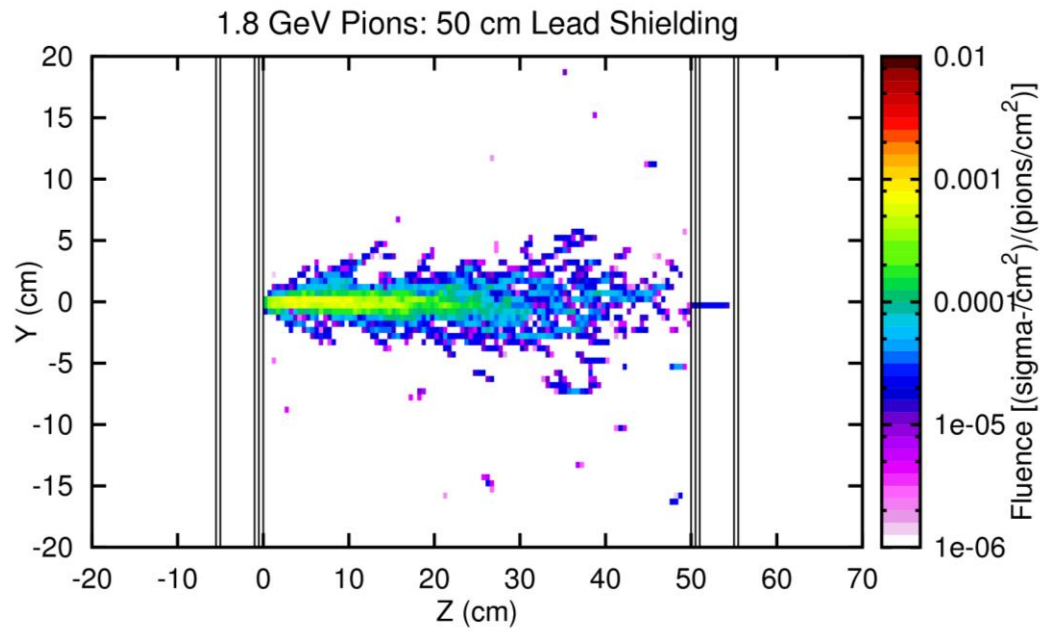


Figure 50. Sigma- fluence in the case of the 50 cm thick lead block per incoming 1.8 GeV pion.

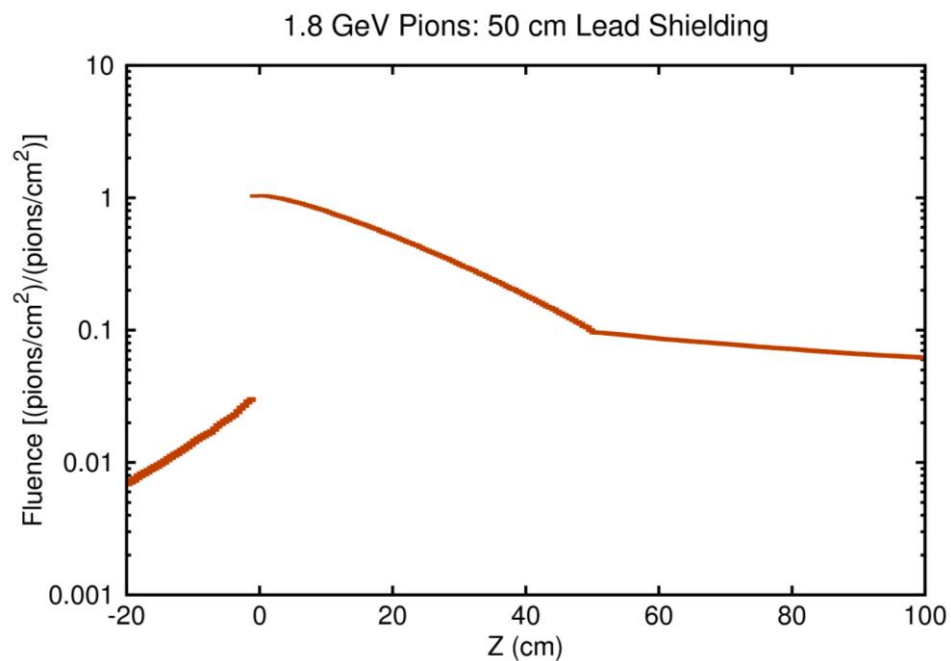


Figure 51. Energy integrated pion fluence as a function of position.

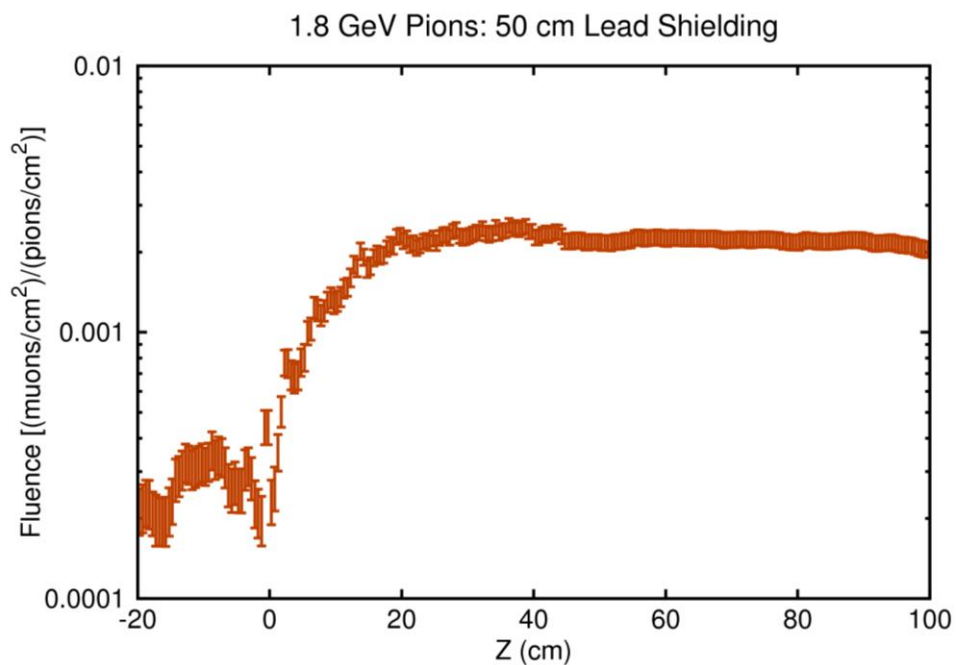


Figure 52. Energy integrated muon fluence as a function of position.

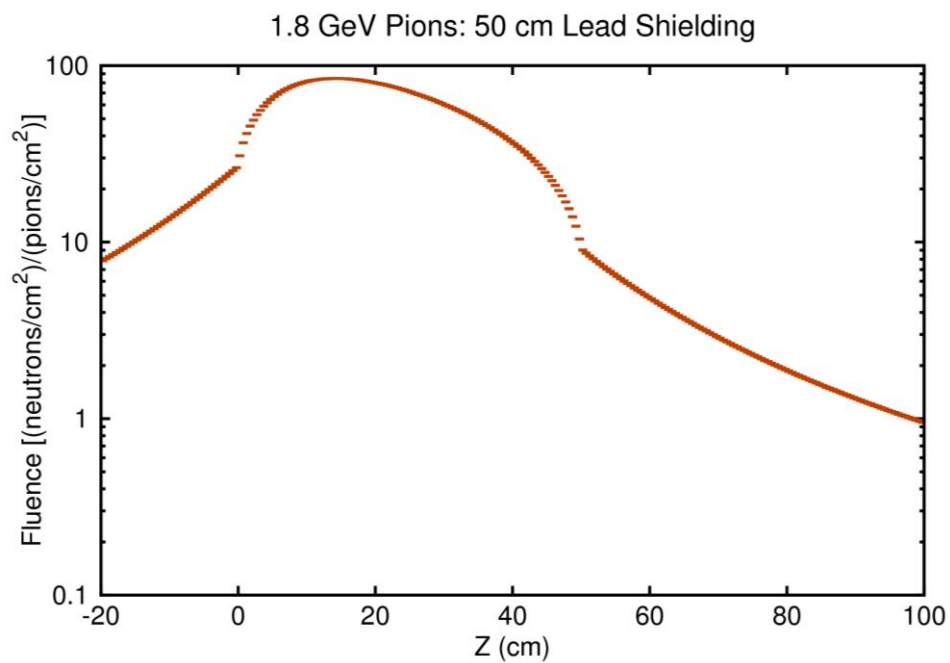


Figure 53. Energy integrated neutron fluence as a function of position.

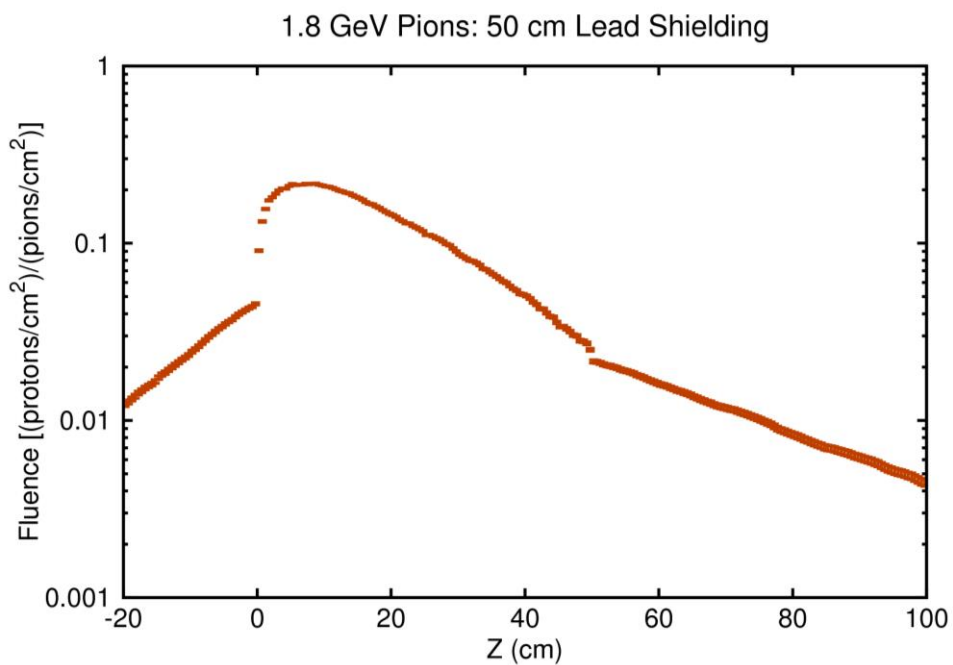


Figure 54. Energy integrated proton fluence as a function of position.

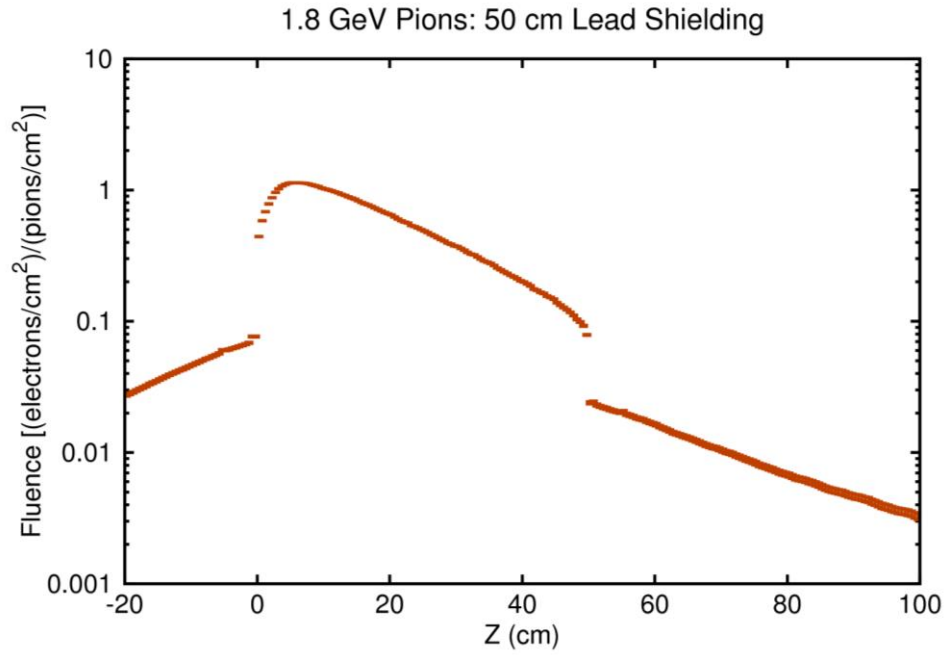


Figure 55. Energy integrated electron fluence as a function of position.

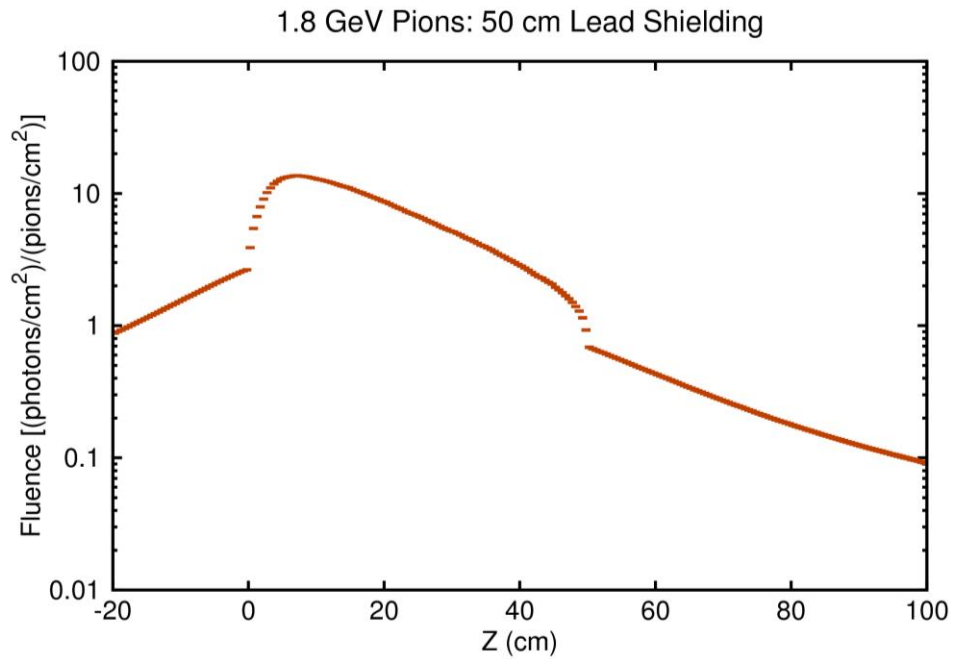


Figure 56. Energy integrated photon fluence as a function of position.

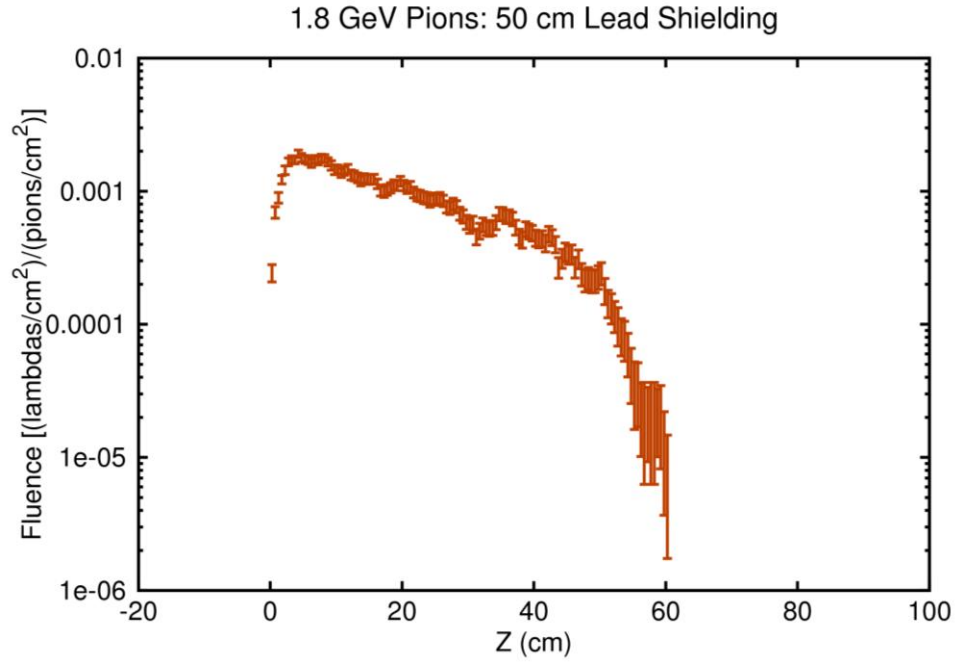


Figure 57. Energy integrated lambda fluence as a function of position.

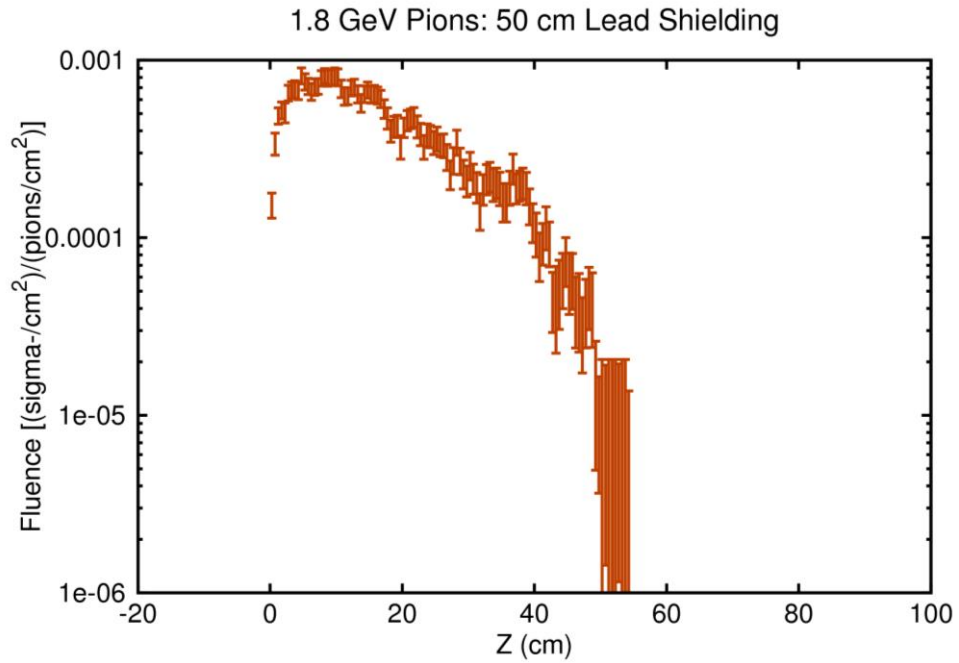


Figure 58. Energy integrated sigma- fluence as a function of position.

The fluences shown in Figures 43-58 are integrated over all secondary particles energies and can be used to calculate the background rates, but, to fully understand the background, it is also important to know the secondary particles energy spectra. In Figures 59-xxx the isoethargic spectra are shown for the secondary particles produced by the shielding in forward and backward directions. The reason for using isoethargic spectra is that the dynamic range of the energies of the secondary particles requires a logarithmic energy scale. For such a scale the area under the isoethargic spectrum curve is proportional to number of particles in a particular energy interval.

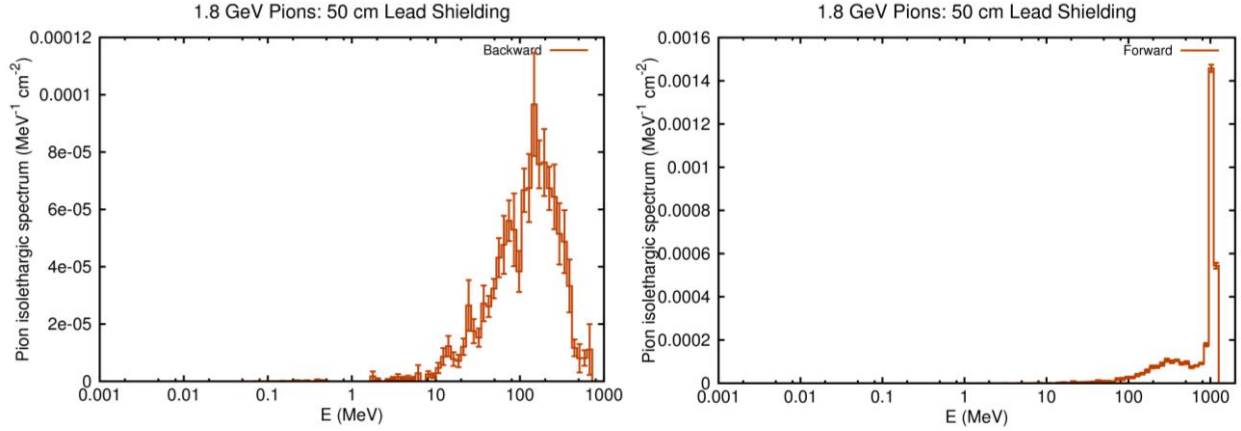


Figure 59. Pion isoethargic spectrum for backward and forward produced pions in a 50 cm thick lead shielding.

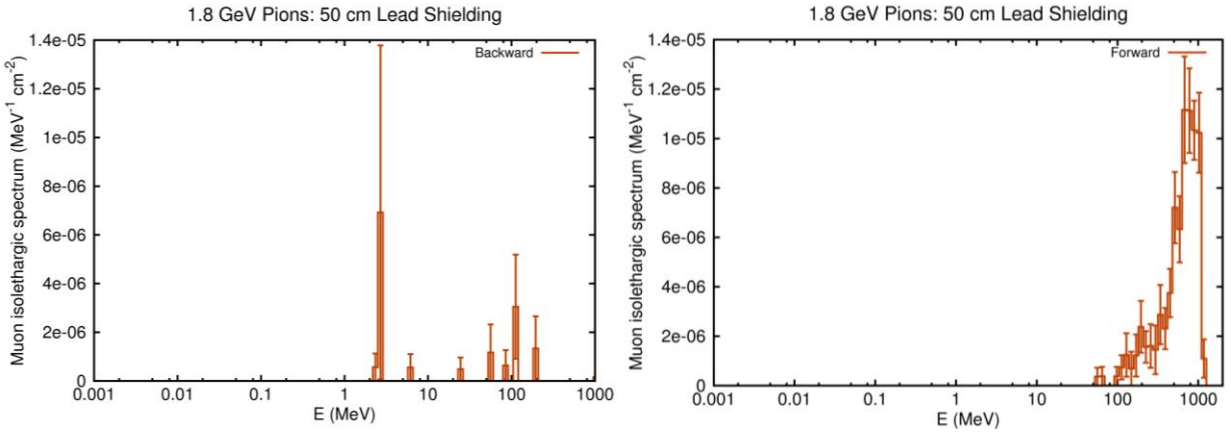


Figure 60. Muon isoethargic spectrum for backward and forward produced muons in a 50 cm thick lead shielding.

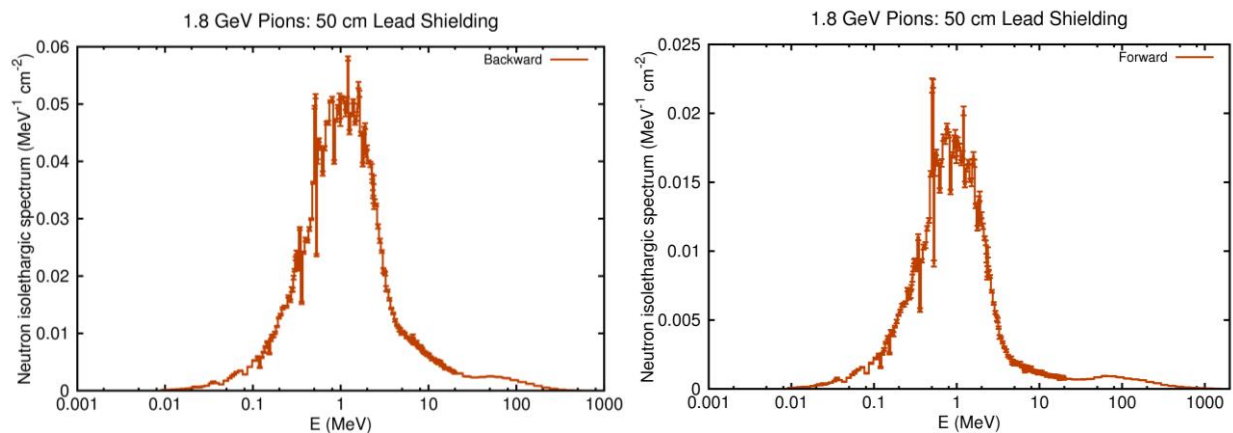


Figure 61. Neutron islethargic spectrum for backward and forward produced neutrons in a 50 cm thick lead shielding.

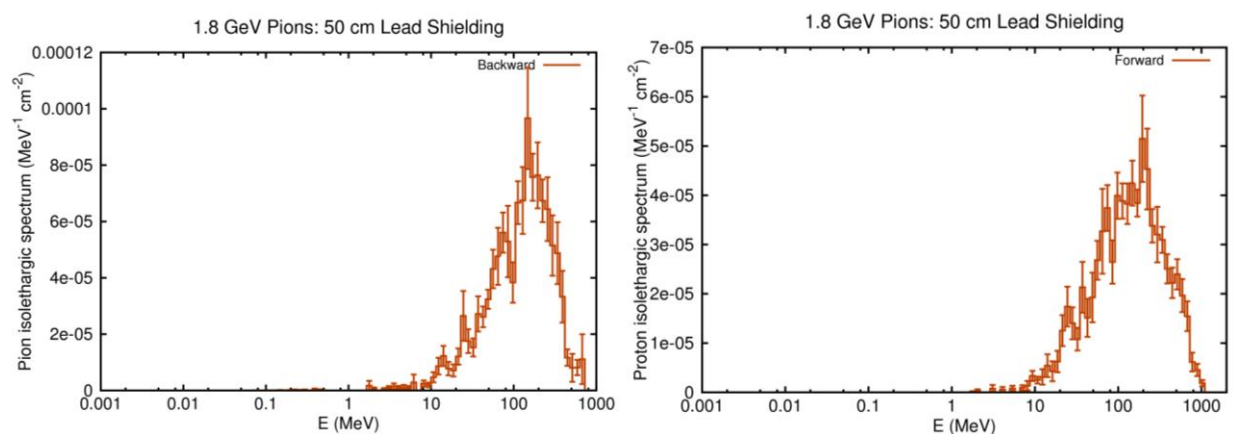


Figure 62. Proton islethargic spectrum for backward and forward produced protons in a 50 cm thick lead shielding.

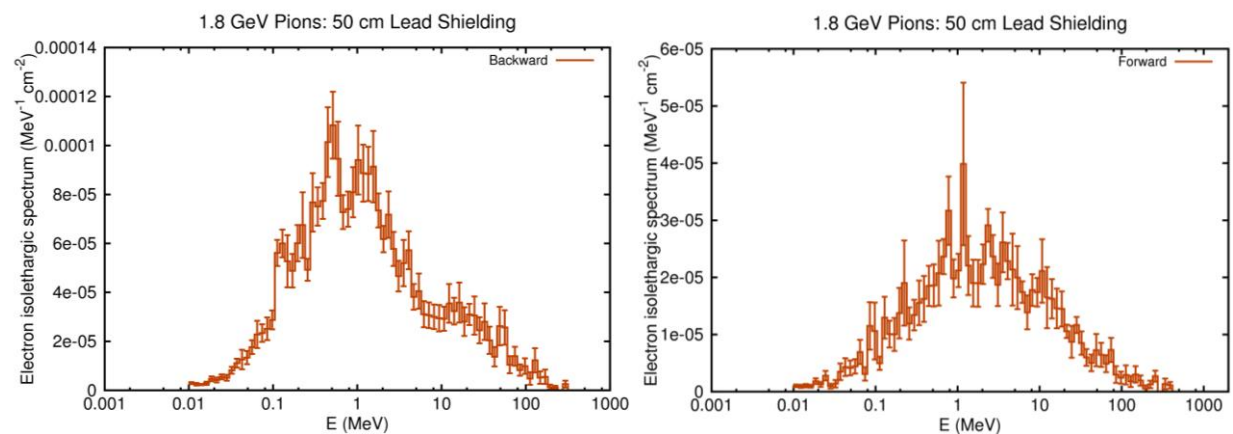


Figure 63. Electron islethargic spectrum for backward and forward produced electrons in a 50 cm thick lead shielding.

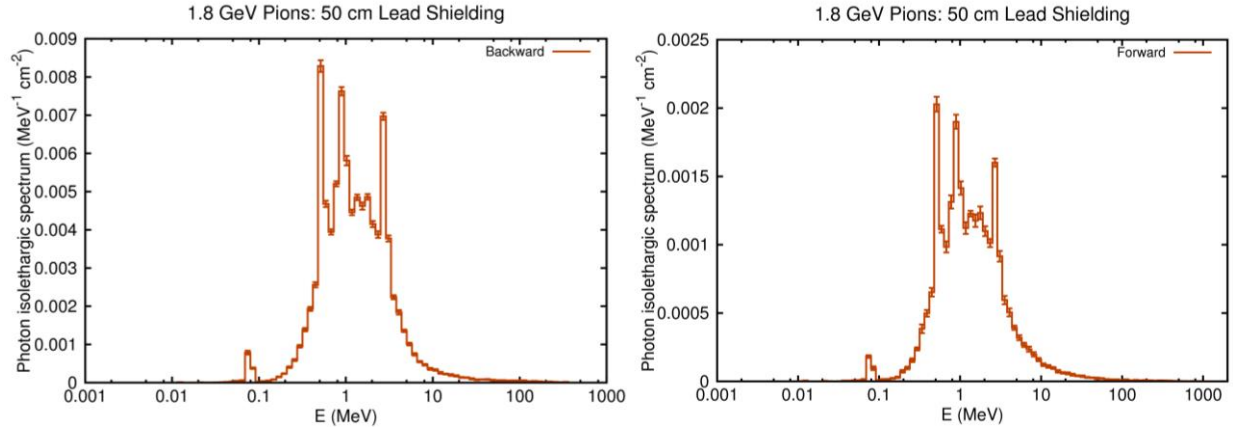


Figure 64. Photon islethargic spectrum for backward and forward produced photons in a 50 cm thick lead shielding.

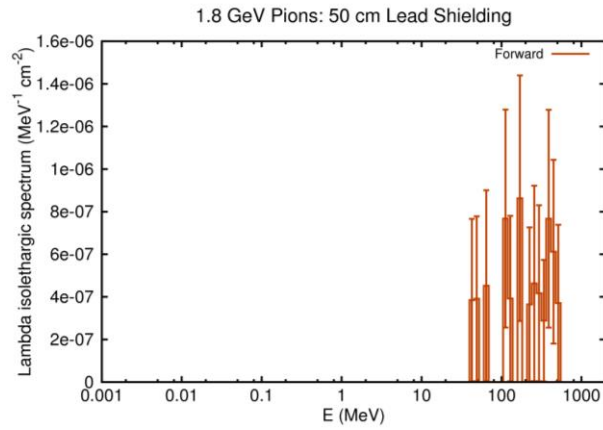


Figure 65. Lambda islethargic spectrum forward produced lambdas in a 50 cm thick lead shielding.

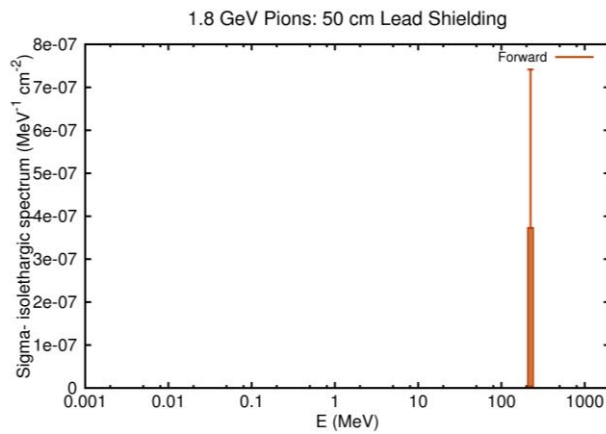


Figure 66. Sigma- islethargic spectrum for forward produced sigma- in a 50 cm thick lead shielding.

In the case of the electrons, the total deposited energy is shown in Figure 67 in units of MeV/cm^3 . The average deposited energy in the entire lead block was 1787 MeV per incoming electron. The fluences integrated over all secondary particles energies are shown in Figures 68-72 and Figures 73-77.

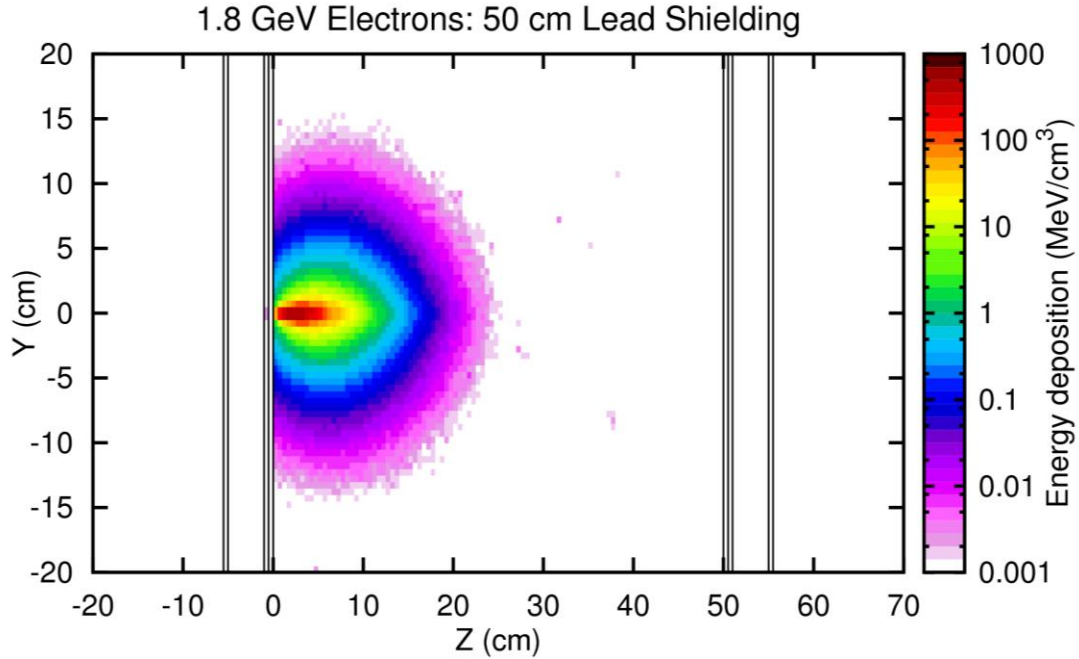


Figure 67. Total deposited energy in the 50 cm thick lead block per incoming 1.8 GeV electron.

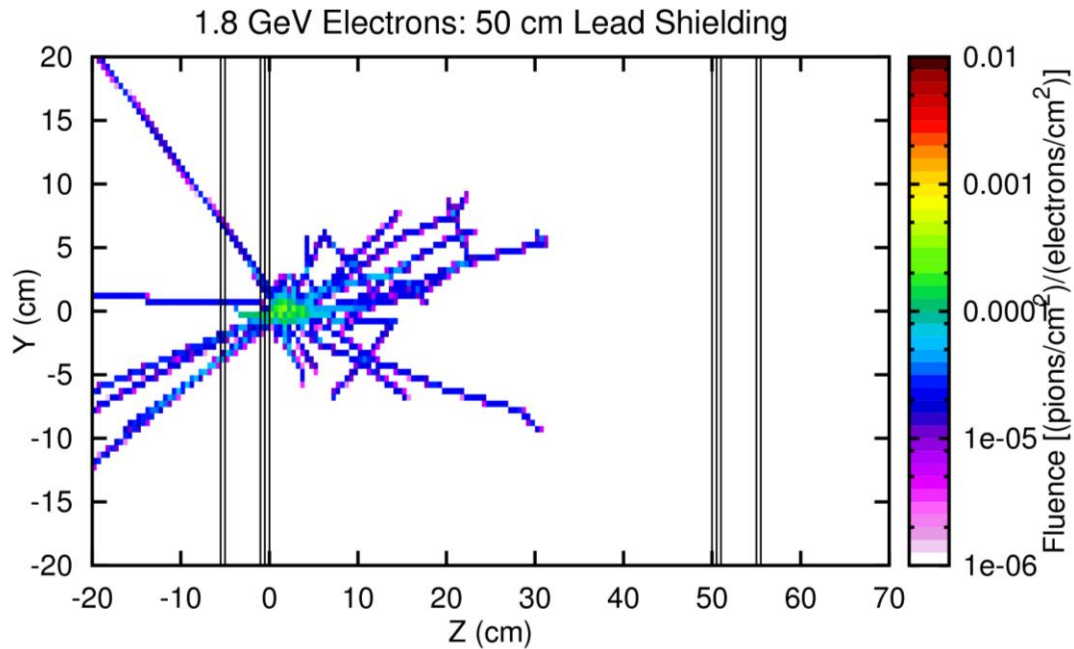


Figure 68. Pion fluence in the case of the 50 cm thick lead block per incoming 1.8 GeV electron.

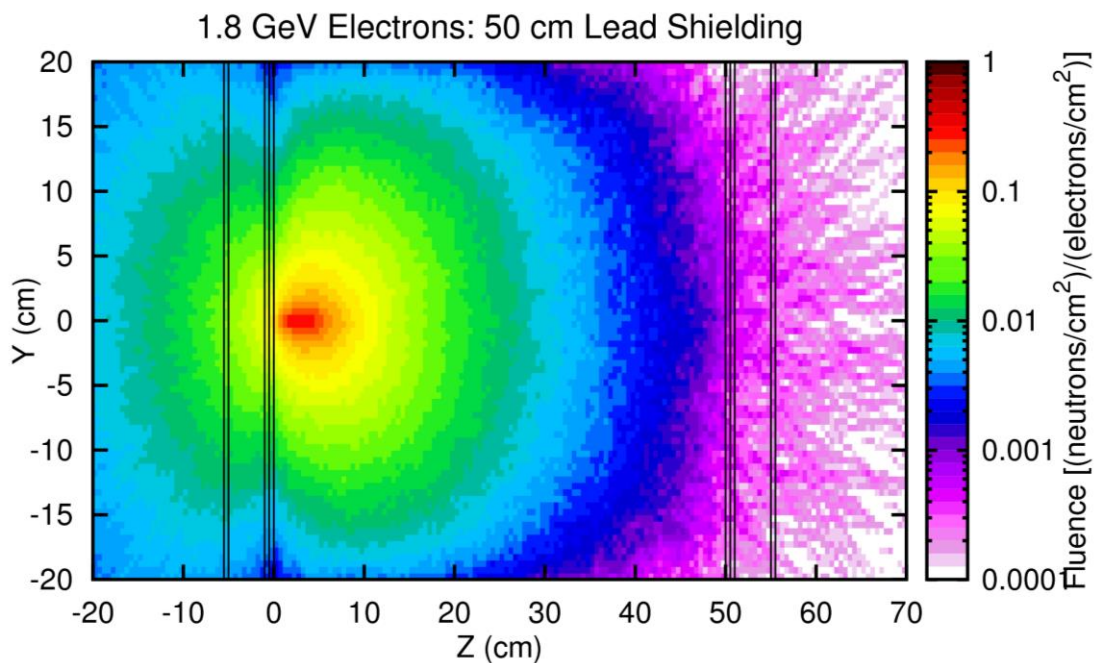


Figure 69. Neutron fluence in the case of the 50 cm thick lead block per incoming 1.8 GeV electron.

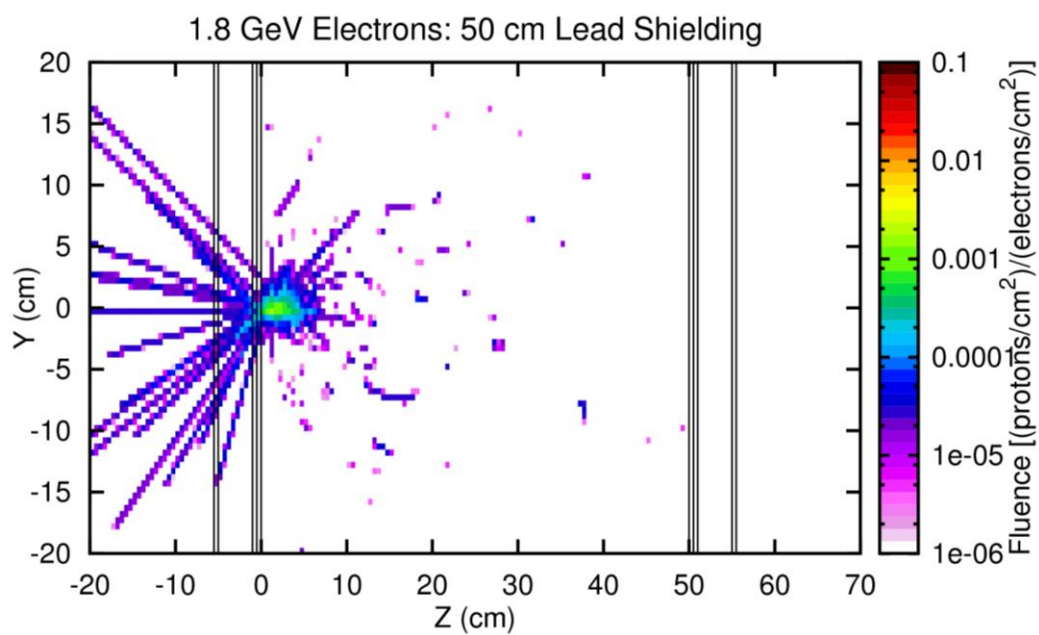


Figure 70. Proton fluence in the case of the 50 cm thick lead block per incoming 1.8 GeV electron.

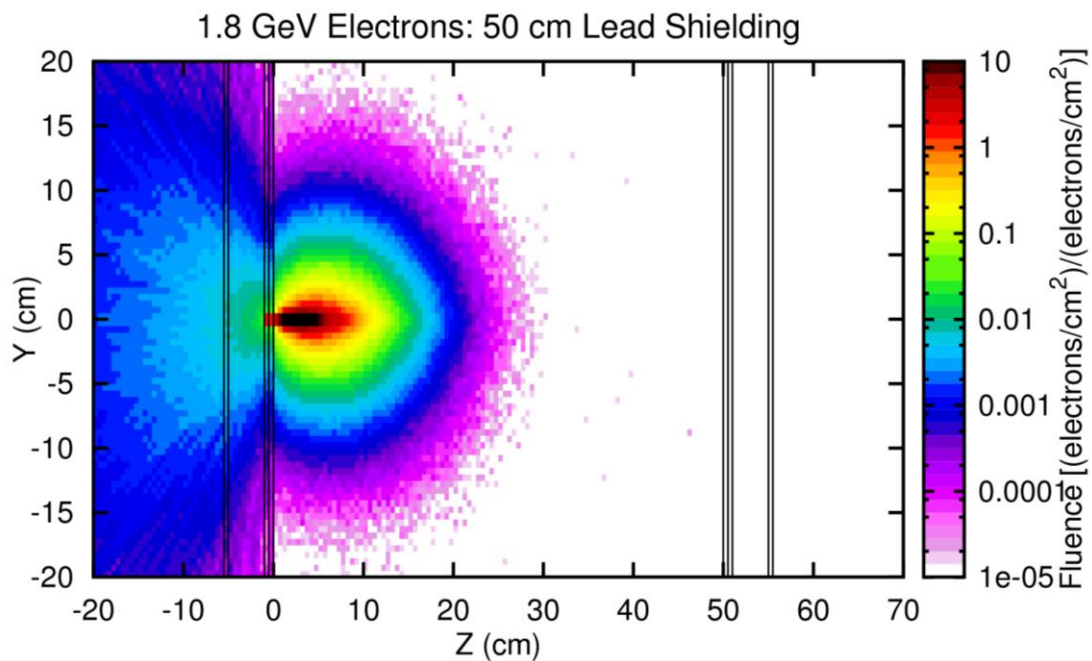


Figure 71. Electron fluence in the case of the 50 cm thick lead block per incoming 1.8 GeV electron.

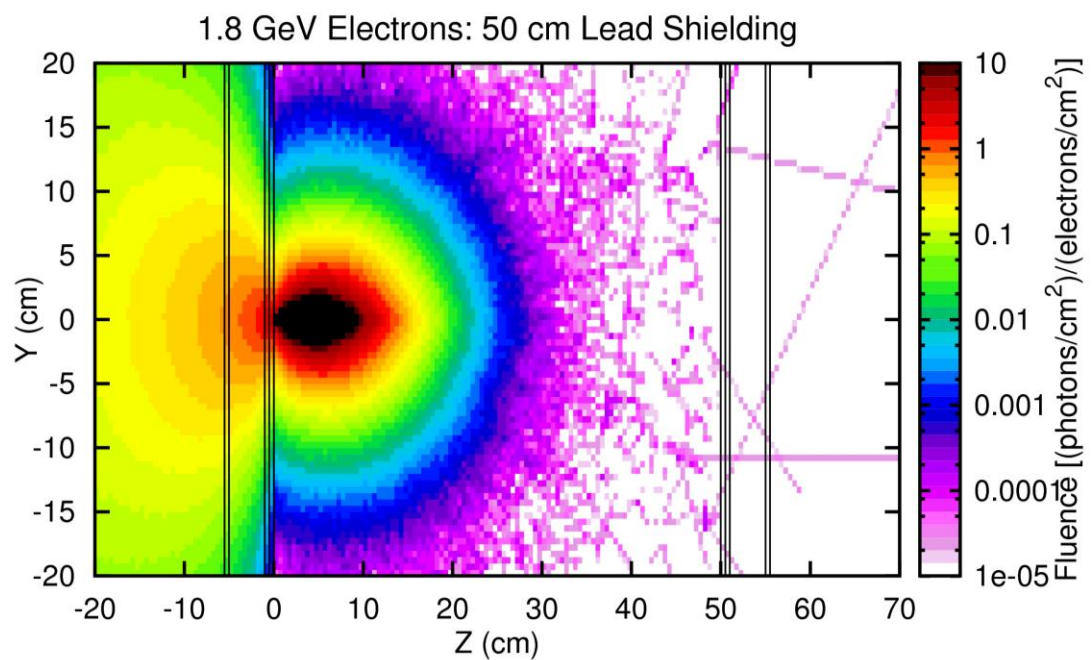


Figure 72. Photon fluence in the case of the 50 cm thick lead block per incoming 1.8 GeV electron.

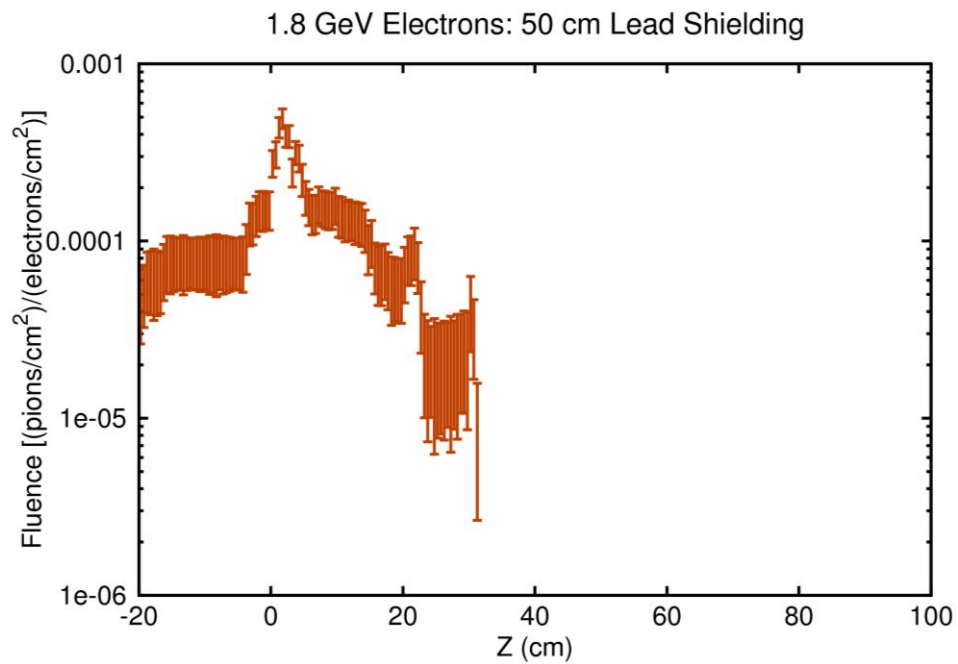


Figure 73. Energy integrated pion fluence as a function of position.

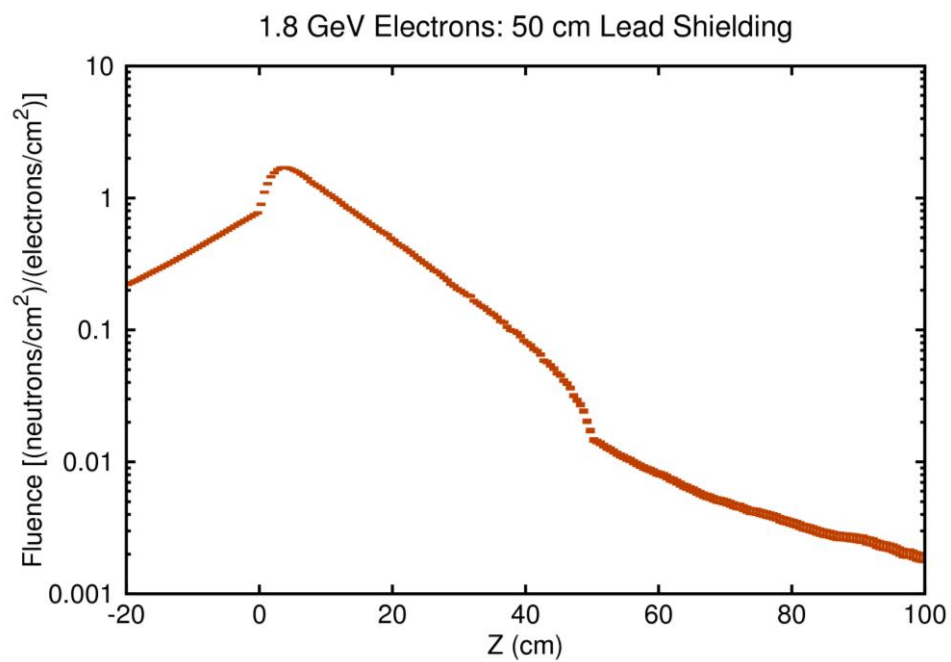


Figure 74. Energy integrated neutron fluence as a function of position.

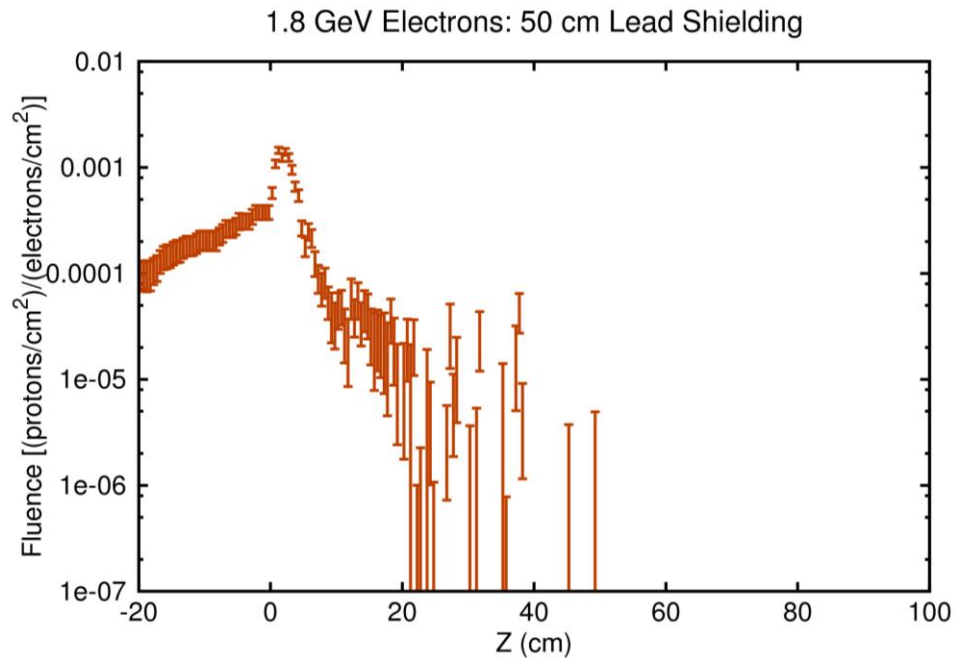


Figure 75. Energy integrated proton fluence as a function of position.

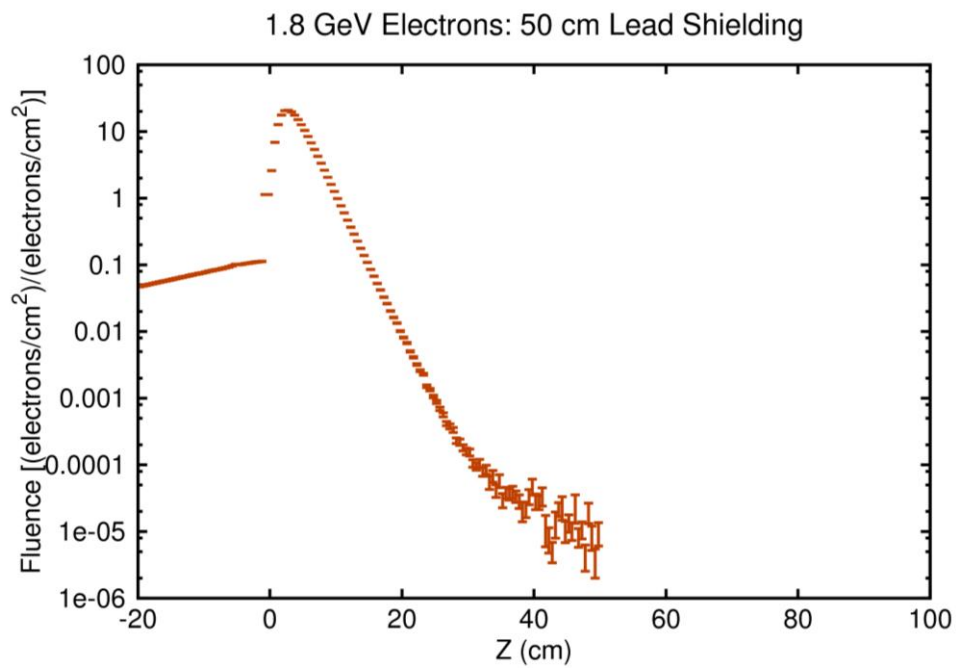


Figure 76. Energy integrated electron fluence as a function of position.

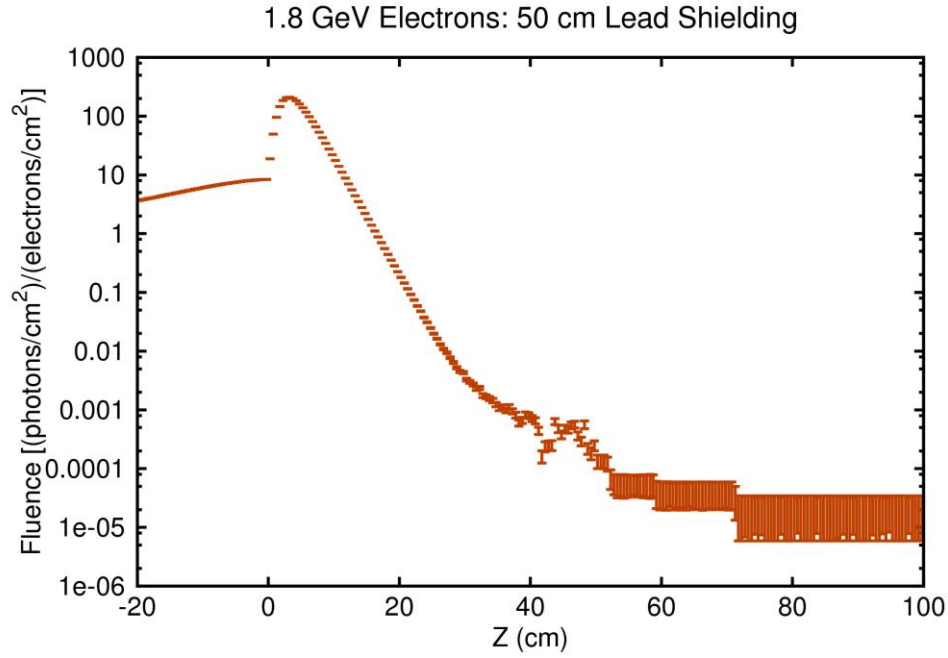


Figure 77. Energy integrated photon fluence as a function of position.

The fluences shown in Figures 68-77 are integrated over all secondary particles energies and can be used to calculate the background rates, but, to fully understand the background, it is also important to know the secondary particles energy spectra. In Figures 78-82 the isoethargic spectra are shown for the secondary particles produced by the shielding in forward and backward directions. The reason for using isoethargic spectra is that the dynamic range of the energies of the secondary particles requires a logarithmic energy scale. For such a scale the area under the isoethargic spectrum curve is proportional to number of particles in a particular energy interval.

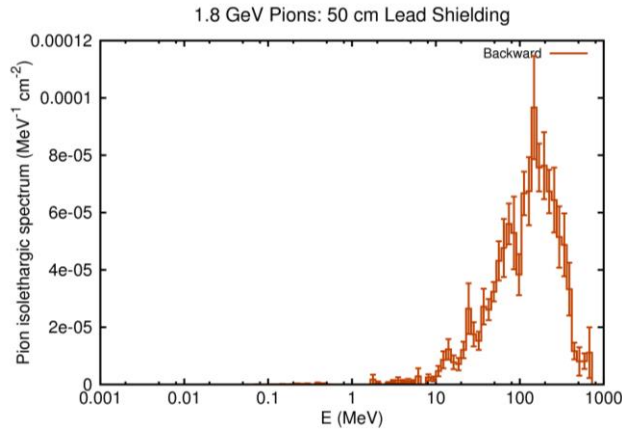


Figure 78. Pion isoethargic spectrum for backward produced pions in a 50 cm thick lead shielding.

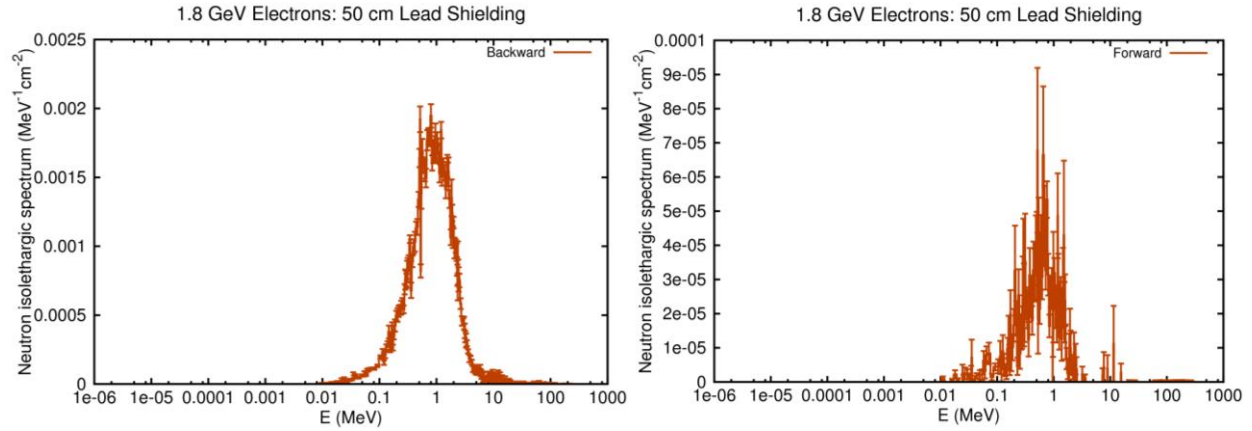


Figure 79. Neutron islethargic spectrum for backward and forward produced neutrons in a 50 cm thick lead shielding.

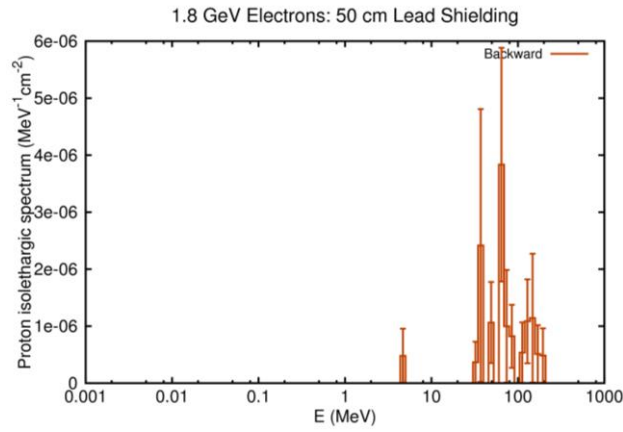


Figure 80. Proton islethargic spectrum for backward produced protons in a 50 cm thick lead shielding.

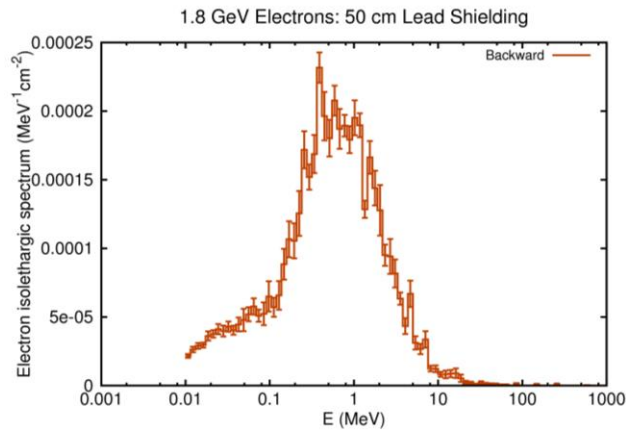


Figure 81. Electron islethargic spectrum for backward produced electrons in a 50 cm thick lead shielding.

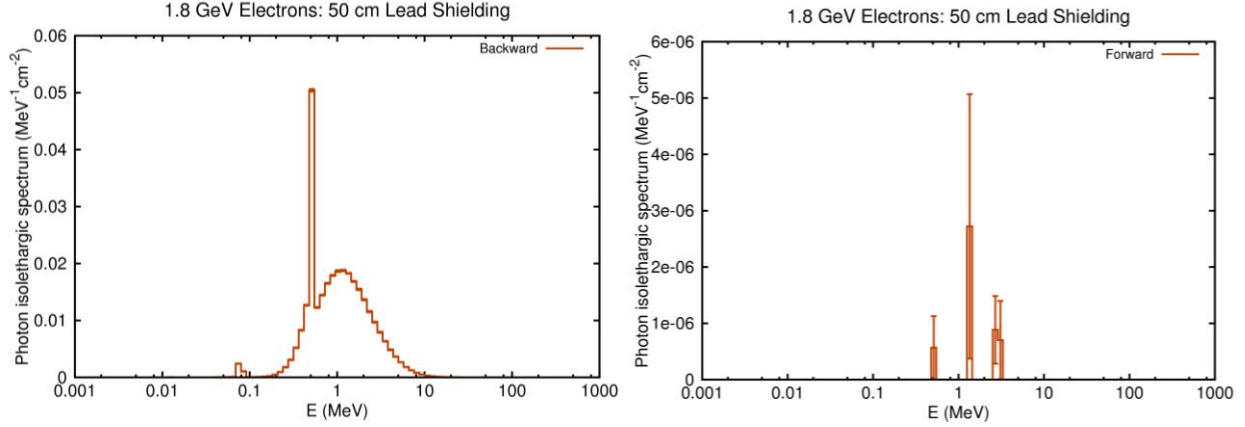


Figure 82. Photon isolethargic spectrum for backward and forward produced photons in a 50 cm thick lead shielding.

VI Summary

The following two tables summarize in more details the results shown in previous figures. Table 2 shows the types, the rates and the energy ranges of the secondary particles produced by the 1.8 GeV electrons in the 20 and 50 cm thick lead shielding in the forward and backward directions. Table 3 shows the types, the rates and the energy ranges of secondary particles produced by the 1.8 GeV pions in the 20 and 50 cm thick lead shielding in the forward and backward directions. The secondary particles rates are obtained assuming the electrons rate of 0.1 GHz/cm^2 and pions rates of $0.1 \times 10^{-3} \text{ GHz/cm}^2$ ($\sim 0.1 \%$ of the electrons rate) as estimate in the Moller experiment proposal [MOLLER2012]. At this stage of the simulation the obtained secondary particles rates are a rough estimate. This is the result of the assumption that, in the energy range of the Moller experiment, the rates are energy independent and that the cross sections of the secondary particles production are energy independent. Luckily, those two assumptions have opposite trends, allowing for the estimates in the tables. It is obvious that with the forthcoming simulations the rates will be improved.

In both tables the energy ranges are shown for the secondary particles except for the pion produced pions where the percentage of the energy unperturbed pions, pions with the original energy, is shown.

While the results in the two tables will help in understanding the effects of the shielding on the pion detector, positioned behind the shielding, and on the main detector system, positioned in front of the shielding, the result can be also used to estimate the secondary particles effects on the main detector system if one decides to put the shielding in front of main detectors.

		Electrons (0.1 GHz/cm ²)			
		Secondary Particles Backward		Secondary Particles Forward	
Lead Shielding:		20 cm	50 cm	20 cm	50 cm
π	Rate (GHz/cm ²)	2 10 ⁻⁵	7.2 10 ⁻⁶	1 10 ⁻⁶	
	Energy (MeV)	5-400			
μ	Rate (GHz/cm ²)	1.6 10 ⁻⁶			
	Energy (MeV)				
n	Rate (GHz/cm ²)	0.08	0.08	0.02	0.0015
	Energy (MeV)	0.01-10		0.01-10	
ρ	Rate (GHz/cm ²)	1.8 10 ⁻⁵	3.8 10 ⁻⁵	1.6 10 ⁻⁶	
	Energy (MeV)	1-200		10-1000	
e^-	Rate (GHz/cm ²)	0.12		2 10 ⁻⁴	
	Energy (MeV)	0.01-10		0.01-10	
γ	Rate (GHz/cm ²)	0.9		0.017	5.2 10 ⁻⁶
	Energy (MeV)	0.01-10		0.01-10	0.1-10
λ	Rate (GHz/cm ²)				
	Energy (MeV)				
Σ^-	Rate (GHz/cm ²)				
	Energy (MeV)				

Table 2. Rates and energy ranges for electron produced secondary particles for different lead thickness.

		Pions (0.1 10 ⁻³ GHz/cm ²)			
		Secondary Particles Backward		Secondary Particles Forward	
Lead Shielding:		20 cm	50 cm	20 cm	50 cm
π	Rate (GHz/cm ²)	3.4 10 ⁻⁶		5 10 ⁻⁵	1 10 ⁻⁵
	Energy (MeV)	1-750		28%	4 %
μ	Rate (GHz/cm ²)	3 10 ⁻⁸		2 10 ⁻⁷	2 10 ⁻⁷
	Energy (MeV)	2-500		15-1800	
n	Rate (GHz/cm ²)	2.3 10 ⁻³	2.6 10 ⁻³	2.1 10 ⁻³	9.2 10 ⁻⁴
	Energy (MeV)	0.1-400		0.1-1000	
ρ	Rate (GHz/cm ²)	5 10 ⁻⁶		1.2 10 ⁻⁵	2.2 10 ⁻⁶
	Energy (MeV)	1-500		1-1500	10-1000
e^-	Rate (GHz/cm ²)	8 10 ⁻⁶		1.7 10 ⁻⁵	2.4 10 ⁻⁶
	Energy (MeV)	0.01-350		0.01-1000	0.01-500
γ	Rate (GHz/cm ²)	2.7 10 ⁻⁴		4 10 ⁻⁴	6.8 10 ⁻⁵
	Energy (MeV)	0.05-100		0.05-100	
λ	Rate (GHz/cm ²)	< 2 10 ⁻⁸		5 10 ⁻⁸	2 10 ⁻⁸
	Energy (MeV)			10-1200	35-650
Σ^-	Rate (GHz/cm ²)	< 2 10 ⁻⁸		3 10 ⁻⁸	5 10 ⁻¹⁰
	Energy (MeV)				

Table 3. Rates and energy ranges for pion produced secondary particles for different lead thickness.

VII Conclusion

In this report detailed studies of the shielding properties and the physical consequences of the shielding of the pion detector are performed for the highest electron and pion energies in the Moller experiment. Effects of the shielding on both, pion detector and the main detector system, are calculated for the lead shielding thicknesses 20 and 50 cm. The type, the energy distributions and the rates of the secondary particles are computed. In addition to help optimize the thickness of the shielding, the results will help to understand the consequences of the background produced by the shielding on both, pion detector and the main detector system, and, therefore, help in the design of the detectors. The result can be also used to estimate the secondary particles effects on the main detector system if one decides to put the shielding in front of main detectors.

References

[BATTISTONI 2007] G. Battistoni, S. Muraro, P.R. Sala, F. Cerutti, A. Ferrari, S. Roesler, A. Fasso`, J. Ranft, “The FLUKA code: Description and benchmarking”, Proceedings of the Hadronic Shower Simulation Workshop 2006, Fermilab 6--8 September 2006, M. Albrow, R. Raja eds., AIP Conference Proceeding 896, 31-49, (2007)

[FERRARI 2005] A. Ferrari, P.R. Sala, A. Fasso`, and J. Ranft, “FLUKA: a multi-particle transport code” CERN-2005-10 (2005), INFN/TC_05/11, SLAC-R-773

[MOLLER2012] MOLLER: Jeferson Lab Experiment E12-09-005:
http://hallaweb.jlab.org/12GeV/Moller/pubs/moller_proposal.pdf